Article type : Original Article

**Title:**

# Arabidopsis inositol phosphate kinases, IPK1 and ITPK1, constitute a metabolic pathway in maintaining phosphate homeostasis

Hui-Fen Kuo,[1] Yu-Ying Hsu,[1] Wei-Chi Lin,[1] Kai-Yu Chen,[1] Teun Munnik,[2] Charles A. Brearley,[3] and Tzyy-Jen Chiou[1]

[1] Agricultural Biotechnology Research Center, Academia Sinica, Taipei 115, Taiwan

[2] Swammerdam Institute for Life Sciences, University of Amsterdam, Science Park 904, 1098XH Amsterdam, The Netherlands

[3] School of Biological Sciences, University of East Anglia, Norwich Research Park, Norwich, Norfolk, NR4 7TJ, U.K.

**Corresponding authors:**

Charles A. Brearley (c.brearley@uea.ac.uk)

School of Biological Sciences, University of East Anglia, U.K.

Tzyy-Jen Chiou (tjchiou@gate.sinica.edu.tw)

Agricultural Biotechnology Research Center, Academia Sinica, Taiwan

**Running Head:** Ins*P* metabolism and $P_i$ homeostasis

**Keywords:** Inositol phosphate, inositol pentakisphosphate 2-kinase (IPK1), inositol 1,3,4-trisphosphate 5/6-kinase 1 (ITPK1), phosphate homeostasis, D/L-inositol 3,4,5,6-tetrakisphosphate, phosphate starvation response, diphosphoinositol pentakisphosphate, phytate biosynthesis, *Arabidopsis thaliana*.

## Summary

Emerging studies have implicated a close link between inositol phosphate (Ins*P*) metabolism and cellular phosphate ($P_i$) homeostasis in eukaryotes; however, whether a common Ins*P* species is deployed as an evolutionarily conserved metabolic messenger to mediate $P_i$ signaling remains unknown. Here, using genetics and Ins*P* profiling combined with $P_i$ starvation response (PSR) analysis in *Arabidopsis thaliana*, we showed that the kinase activity of inositol pentakisphosphate 2-kinase (IPK1), an enzyme required for phytate (inositol hexakisphosphates; Ins$P_6$) synthesis, is indispensable for maintaining $P_i$ homeostasis under $P_i$-replete conditions, and inositol 1,3,4-trisphosphate 5/6-kinase 1 (ITPK1) plays an equivalent role. Although both *ipk1-1 and itpk1* mutants exhibited

decreased levels of Ins$P_6$ and diphosphoinositol pentakisphosphate (PP-Ins$P_5$; Ins$P_7$), disruption of another ITPK family enzyme, ITPK4, which correspondingly caused depletion of Ins$P_6$ and Ins$P_7$, did not display similar $P_i$-related phenotypes, which precludes these Ins*P* species as effectors. Notably, the level of D/L-Ins(3,4,5,6)$P_4$ was concurrently elevated in both *ipk1-1* and *itpk1* mutants, which showed a specific correlation to the misregulated $P_i$ phenotypes. However, the level of D/L-Ins(3,4,5,6)$P_4$ is not responsive to $P_i$ starvation that instead manifests a shoot-specific increase in Ins$P_7$ level. This study demonstrates a more nuanced picture of the intersection of Ins*P* metabolism and $P_i$ homeostasis and PSR than has previously been elaborated and additionally establishes intermediate steps to phytate biosynthesis in plant vegetative tissues.

## Introduction

Elemental phosphorous (P) in its oxidized form, phosphate ($PO_4^{3-}$; $P_i$), is essential to all life. As a component of nucleic acids, proteins, phospholipids and numerous intermediary metabolites, $P_i$ is key to energy metabolism and signal transduction. Plants preferentially acquire P in the form of $P_i$ from the rhizosphere, where $P_i$ is often limiting owing to its sorption to soil particles and leaching (Holford, 1997). As an adaptation to fluctuating external $P_i$ concentrations, plants have evolved intricate regulatory mechanisms to maintain cellular $P_i$ homeostasis in vegetative tissue in order to coordinate growth, development, and reproduction, whereas in seeds, $P_i$ is reserved in phytate (inositol hexakisphosphate, Ins$P_6$) that accumulates to several percentage dry weight (Raboy, 1997). In response to $P_i$ deficiency, plants initiate a systematic response, termed the $P_i$-starvation response (PSR), which involves transcriptional, metabolic, and morphological reprogramming, to enhance $P_i$ uptake, allocation, remobilization, and conservation (Rouached *et al.*, 2010; Yang and Finnegan, 2010). Under $P_i$-replete or -replenishment conditions, plant cells relieve PSR and store excess $P_i$ in the vacuole to avoid cellular toxicity as a result of cytosolic $P_i$ surge (Müller *et al.*, 2004; Lin *et al.*,

2013; Liu *et al.*, 2015; Liu *et al.*, 2016). How plant cells perceive external and cellular $P_i$ status to maintain $P_i$ homeostasis remains elusive despite reports of multiple factors proposed to be signaling molecules, including sugar, phytohormones, microRNAs, Ins*P*s and $P_i$ *per se* (Martin *et al.*, 2000; Franco-Zorrilla *et al.*, 2005; Liu *et al.*, 2005; Bari *et al.*, 2006; Chiou *et al.*, 2006; Chiou and Lin, 2011; Puga *et al.*, 2014; Wang *et al.*, 2014).

Inositol phosphates (Ins*P*s) are metabolites of variable phosphorylation on a carbohydrate core, inositol, and are present in all eukaryotes. They are synthesized by evolutionarily conserved enzymes (Irvine and Schell, 2001) and play important roles in diverse cellular processes by functioning as structural and functional cofactors, regulators, and second messengers (Shears *et al.*, 2012). According to the definition of a 'signal', being that of agonist-responsive change in concentration that is recognized by a defined receptor (Shears *et al.*, 2012), only very few Ins*P*s can be considered true signaling molecules, including Ins(1,4,5)$P_3$ in the context of $Ca^{2+}$ signaling (Berridge, 2009) and Ins(3,4,5,6)$P_4$ as a regulator of the conductance of the $Ca^{2+}$-activated chloride channels (Vajanaphanich *et al.*, 1994; Shears *et al.*, 2012). In plants, Ins*P*s have been hypothesized to mediate signaling of multiple physiological processes, including stomatal closure, gravitropism, drought tolerance, and defense (Lemtiri-Chlieh *et al.*, 2000; Lemtiri-Chlieh *et al.*, 2003; Perera *et al.*, 2006; Mosblech *et al.*, 2008; Murphy *et al.*, 2008; Perera *et al.*, 2008; Laha *et al.*, 2015); however, their roles as signaling messengers in most cases have not been assessed extensively.

The first elaboration of the involvement of Ins*P*s in eukaryotic $P_i$ homeostasis was revealed when a rabbit cDNA clone was shown to stimulate $P_i$ uptake when ectopically expressed in Xenopus oocytes (Norbis *et al.*, 1997). This so-called $P_i$ uptake stimulator ($P_i$US) was identified to encode an Ins$P_6$ kinase (IP6K) that converts Ins$P_6$ to diphosphoinositol pentakisphosphates (PP-Ins$P_5$ or Ins$P_7$) (Norbis *et al.*, 1997; Schell *et al.*, 1999). In yeast, disruption of multiple enzymes responsible for biosynthesis of Ins*P*s and diphosphoinositol phosphates (PP-Ins*P*s) (e.g., Plc1p, Arg82p, and Kcs1p) led to constitutive activation of a $P_i$ starvation-responsive phosphatase-coding gene, Pho5, under

$P_i$-replete conditions (Auesukaree *et al.*, 2005). Subsequent work showed that the synthesis of Ins*P*$_7$ by the other family of PP-Ins*P* kinases (Vip1/PPIP5K), Vip1, is stimulated by $P_i$ starvation (Lee *et al.*, 2007) and Ins*P*$_7$ binds to Pho81, causing inhibition of the Pho80-Pho85 cyclin-cyclin–dependent kinase complex and unphosphorylation of the Pho4 transcription factor. The resulting reduction in phosphorylation of Pho4 localizes this protein to the nucleus, where it activates $P_i$ starvation-inducible genes (Lee *et al.*, 2007; Lee *et al.*, 2008). The synthesis of PP-Ins*P*s is also metabolically linked to the synthesis of the main intracellular $P_i$ storage molecule, a linear chain of polyphosphate (polyP), and the yeast IP6K mutant, *kcs1*Δ, fails to accumulate polyP (Auesukaree *et al.*, 2005; Lonetti *et al.*, 2011).

Cellular adenylate energy is influenced by $P_i$ availability and PP-Ins*P* synthesis (Boer *et al.*, 2010; Szijgyarto *et al.*, 2011; Choi *et al.*, 2017) and itself regulates the synthesis of PP-Ins*P* (Voglmaier *et al.*, 1996; Saiardi *et al.*, 1999; Wundenberg *et al.*, 2014). Together with the genetic and molecular evidence described previously, PP-Ins*P*s have been proposed as metabolic messengers that mediate $P_i$ signaling. This hypothesis is further supported by structural and biochemical analyses demonstrating that Ins*P*s and PP-Ins*P*s bind to an evolutionarily conserved SYG1/PHO81/XPR1 (SPX) domain present in proteins that play key roles in $P_i$ sensing and transport, with PP-Ins*P*s showing the highest binding affinity (at sub-micromolar concentrations for yeast and animal protein) (Secco *et al.*, 2012; Secco *et al.*, 2012; Wild *et al.*, 2016). Disruption of Ins*P*/PP-Ins*P* binding sites in the SPX domain impaired yeast vacuolar transporter chaperone (VTC)-dependent polyP synthesis and failed to complement $P_i$-related phenotypes of the Arabidopsis *phosphate 1* (*pho1*) mutant (Wild *et al.*, 2016). Despite the wealth of current investigation, the evidence for PP-Ins*P*s as evolutionally conserved messengers in eukaryotic $P_i$ signaling is scattered, confounded by the absence of Pho80-Pho85-Pho81 homologs in other eukaryotic organisms and the contradictory responses of Ins*P*$_7$ levels to $P_i$ starvation reported in yeast (Lee *et al.*, 2007; Wild *et al.*, 2016) as well as the presence of a Vip1-independent PHO signaling pathway (Choi *et al.*, 2017).

In plants, a contemporary implication of Ins*P* metabolism in regulation of $P_i$ homeostasis comes from a study in which genetic disruption of the kinase responsible for Ins$P_6$ synthesis, inositol pentakisphosphate 2-kinase (IPK1), causes excessive $P_i$ accumulation (Stevenson-Paulik *et al.*, 2005) as a result of elevated $P_i$ uptake/allocation activities and activation of a subset of $P_i$ starvation-responsive genes (PSR genes) under $P_i$-replete conditions (Kuo *et al.*, 2014). In addition to decreased Ins$P_6$ level, *ipk1* mutation causes a significant change in Ins*P* composition, including accumulation of lower phosphorylated Ins*P* species (e.g., Ins$P_3$, Ins$P_4$ and Ins$P_5$) and decreased levels of PP-Ins*P*s [Ins$P_7$ and Ins$P_8$ (*bis*diphosphoinositol tetrakisphosphate)] (Stevenson-Paulik *et al.*, 2005; Laha *et al.*, 2015). The mechanism of IPK1 modulating $P_i$ homeostasis and whether Ins*P*s play a role in $P_i$-starvation signaling in plants is currently unknown.

As compared with the situation in other eukaryotic organisms, the investigation of biosynthesis of Ins*P*s and their composition in the vegetative tissues of plants is necessarily more complicated than in other eukaryotes due to the presence of complex gene families of Ins*P* biosynthesis enzymes. Mammalian Ins*P* metabolism is dominated by receptor-coupled activation of phospholipase C (PLC) and subsequent metabolic conversion of Ins(1,4,5)$P_3$ to multiple higher and lower Ins*P*s (Irvine and Schell, 2001), but few plant studies offer detailed identification of Ins*P* species in vegetative tissues due to the limited levels of labeling achieved with *myo*-[$^3$H]inositol. Nevertheless, specific short-term non-equilibrium labeling with [$^{32}$P]$P_i$ has afforded a metabolic test capable of distinguishing the order in which phosphates are added to the inositol core (Stephens and Downes, 1990; Stephens and Irvine, 1990; Whiteford *et al.*, 1997) and applied to vegetative tissues of plants that revealed a 'lipid-independent' pathway of Ins$P_6$ synthesis (Brearley and Hanke, 1993; Brearley *et al.*, 1997).

Here, using reverse genetics and Ins*P* profiling by [$^3$H]inositol and [$^{32}$P]$P_i$ labelling, we show that maintenance of $P_i$ homeostasis in plants under $P_i$-replete conditions depends on the kinase activity of IPK1 and an additional inositol 1,3,4-trisphosphate 5/6-kinase ITPK1. Profile comparison of Ins*P*s between *ipk1-1*, *itpk1*, and another mutant defective in Ins$P_6$ synthesis, *itpk4*, reveals a correlation

between elevated D/L-Ins(3,4,5,6)$P_4$ [Ins(1,4,5,6)$P_4$ and/or Ins(3,4,5,6)$P_4$] level and activation of $P_i$ uptake and PSR gene expression. However, the Ins*P* profile in response to $P_i$ starvation is distinct from that of the *ipk1-1* and *itpk1* mutants and marked a shoot-specific increase in Ins$P_7$ level accompanied by ATP increase. Our study reveals a complex relationship between Ins*P* metabolism and $P_i$ homeostasis in plants and identifies ITPK4 as a key enzyme in generating Ins$P_4$ precursors for phytate biosynthesis.

## Results

### Kinase activity of *IPK1* is required for maintenance of $P_i$ homeostasis

We previously demonstrated $P_i$ overaccumulation in *ipk1-1* mutants associated with activation of PSR genes involved in $P_i$ uptake, allocation, remobilization, and signaling (Kuo *et al.*, 2014). Because Ins*P* kinases have been implicated in transcriptional regulation independent of their catalytic activities (Bosch and Saiardi, 2012; Xu *et al.*, 2013; Xu *et al.*, 2013) , we examined whether regulation of $P_i$ homeostasis by *IPK1* is kinase-dependent. We constructed two forms of IPK1 bearing mutations in conserved kinase motifs (Stevenson-Paulik *et al.*, 2005) (Figure S1a) at Lys168 (*IPK1*$^{K168A}$) or Asp368 (*IPK1*$^{D368A}$), both shown to cause loss of kinase activity *in vitro* (Gonzalez *et al.*, 2010). The expression of wild-type (WT) IPK1 complemented low Ins$P_6$ content in *ipk1-1* seeds, whereas Ins$P_6$ levels in seeds of transgenic lines expressing either of the two point-mutated forms of *IPK1* remained as low as that in *ipk1-1* seeds (Figure 1a). These point-mutated *IPK1* forms were expressed both at the transcriptional and translational levels (Figures 1b and S1b), with subcellular protein localization in the cytosol and nucleus, similar to the WT *IPK1* (Figure S1c). These results indicated that Lys168 and Asp368 are required for kinase activity of *IPK1 in vivo*.

In contrast to WT *IPK1*, which was able to restore the $P_i$ content of the *ipk1-1* mutant to the WT level, both kinase-inactive *IPK1* forms failed to complement excessive $P_i$ accumulation and PSR gene activation in *ipk1-1* (Figure 1b, c). Therefore, the kinase activity of *IPK1* is required for regulation of $P_i$ homeostasis. In addition to regulating $P_i$ content, the kinase activity of *IPK1* is also required for root system architecture (RSA), because neither of the kinase-inactive IPK1 proteins complemented the PSR-like RSA phenotypes (i.e., reduced primary root and enhanced lateral root growth) of *ipk1-1* (Figure S1d).

**Misregulation of $P_i$ homeostasis in *ipk1-1* is not caused by defective Ins$P_6$-mediated mRNA export**

In yeast, Ins$P_6$ is required for mRNA export by activating the RNA-dependent ATPase activity of DEAD-box protein 5 (Dbp5p) in conjunction with GLFG lethal 1 (Gle1p), and mutations in *ipk1* and *gle1* resulted in mRNA retention in the nucleus and temperature-sensitive growth defects (York *et al.*, 1999; Alcazar-Roman *et al.*, 2006). A conserved mechanism was recently reported in Arabidopsis, and part of the growth defect of *ipk1-1* is attributed to compromised mRNA export due to reduced level of Ins$P_6$ (Lee *et al.*, 2015). To address whether defective mRNA export in the *ipk1-1* mutant is a cause of the misregulation of $P_i$ homeostasis, we examined $P_i$-related phenotypes of the mRNA export mutants reported (Lee *et al.*, 2015). As shown in Figure S2, the loss-of-function mutation in the Dbp5 homologous gene *LOW EXPRESSION OF OSMOTICALLY RESPONSIVE GENES 4* (*LOS4*), and inducible *GLE1* RNAi lines exhibited WT $P_i$ content (Figure S2a,b) and PSR gene expression (Figure S2c). Furthermore, expression of variants of Gle1 (IS1 and IS2), which exhibit increased Ins$P_6$ sensitivity to LOS4 stimulation and improved growth defects of *ipk1-1* (Lee *et al.*, 2015), did not reduce $P_i$ content or suppress PSR gene activation of the *ipk1-1* mutant (Figure S2c, d). These results suggest that misregulation of $P_i$ homeostasis in *ipk1-1* is not caused by defective mRNA export due to reduced Ins$P_6$ level.

**Genetic dissection of the roles for Ins*P* and PP-Ins*P* biosynthesis enzymes in $P_i$ homeostasis regulation**

The dependence of $P_i$ homeostasis on the kinase activity of IPK1 suggested that the PSR activation signal is derived from Ins*P* biosynthesis. To dissect which step(s) of Ins*P* and PP-Ins*P* biosynthesis controls this signal, we examined $P_i$-related phenotypes of mutants defective in several Ins*P* and PP-Ins*P* biosynthesis enzymes previously characterized in Arabidopsis, including *myo*-inositol-3-phosphate synthases (MIPS1-3) (Torabinejad and Gillaspy, 2006), Ins(1,4,5)$P_3$ 6-/3-kinases (inositol phosphate multikinases; IPK2α and IPK2β) (Stevenson-Paulik *et al.*, 2002), Ins(1,3,4)$P_3$ 5-/6-kinase enzymes (inositol phosphate tris/tetrakisphosphate kinases; ITPK1-4) (Wilson and Majerus, 1997; Sweetman *et al.*, 2007), PP-Ins*P* synthesizing enzyme PPIP5K (VIP1/VIH2 and VIP2/VIH1) (Desai *et al.*, 2014; Laha *et al.*, 2015), and a mutant of an Ins$P_6$ transporter, multidrug resistance-associated protein 5 (MRP5) (Nagy *et al.*, 2009). T-DNA insertional mutants were obtained and confirmed by RT-PCR to be null mutants (Table S1 and Figure S3a, b).

Morphologically, none of the mutants displayed growth defects as severe as *ipk1-1* (stunted growth and leaf necrosis), although *mips1*, *itpk1* and *mrp5-2* mutants were smaller than the WT (Figure 2a). The leaf epinasty and PSR-like RSA phenotypic characteristics of *ipk1-1* mutants (Stevenson-Paulik *et al.*, 2005; Kuo *et al.*, 2014) were observed in *itpk1* and *mrp5-2* mutants (Figures 2a and S3c, d) (Kuo *et al.*, 2014). Analysis of $P_i$ content in the shoot tissues revealed that only *itpk1* accumulated excessive $P_i$ comparable to *ipk1-1* (Figure 2b), and this phenotype persisted to the mature stage (Figure S3e). Mild but significantly elevated $P_i$ content was observed in *mrp5-2* seedlings but was no longer seen at the mature stage (Figures 2b and S3e). Consistent with the elevated $P_i$ content, *itpk1* exhibited elevated uptake of $P_i$ activity comparable with that of *ipk1-1*, whereas all other mutants showed WT activities (Figure 2c-f). The excessive $P_i$ accumulation in *itpk1* mutants could be restored to the WT level by ectopic expression of a genomic construct of the *ITPK1* sequence (Figure S4a), which confirms a role for ITPK1 in regulating $P_i$ homeostasis.

In addition to decreased Ins$P_6$ level, levels of Ins$P_7$ and Ins$P_8$ are also reduced in *ipk1-1* mutants (Laha *et al.*, 2015). We therefore examined whether PP-Ins*P*s also play a role in the regulation of $P_i$ homeostasis or PSR in plants. Two families of kinases, IP6K and Vip/PPIP5K, are involved in PP-Ins*P* synthesis in eukaryotes (Wundenberg *et al.*, 2014); however, only Vip1/PPIP5K homologs are identified in plants and shown to be responsible for Ins$P_8$ but not Ins$P_7$ synthesis in Arabidopsis (Mulugu *et al.*, 2007; Desai *et al.*, 2014; Laha *et al.*, 2015). We analyzed mutants defective in each of the two Arabidopsis Vip1/PPIP5K homologs, AtVIP1/VIH2 and AtVIP2/VIH1, and observed slightly decreased $P_i$ content in two alleles of *atvip1* mutants (abbreviated as *vip1-1* and *vip1-2*) with T-DNA disrupting the phosphatase-like domain but not in the alleles disrupted in the ATP-grasp kinase domain (*vih2-3* and *vih2-4*) (Figure S3b) (Laha *et al.*, 2015). Three *atvip2* mutants (abbreviated as *vip2-1*, *vip2-2* and *vih1*) did not show $P_i$-content phenotype, but *vip1-2 vip2-1* double mutants exhibited lower $P_i$ content comparable to the *vip1-2* single mutant (Figures 2b and S3e), which suggests a dominant role for *vip1* mutation in determining this phenotype. Despite the lower $P_i$ content, $P_i$ uptake and root-to-shoot allocation activity did not change in the *vip1-1* or *vip1-2* mutants (Figures 2f and S5a). Furthermore, the expression of PSR genes under $P_i$-replete conditions and the magnitude of PSR gene activation in response to $P_i$ starvation in the *vip1/vih2* and *vip2/vih1* mutants were similar to that in the WT (Figure S5b, c). The cause of reduced $P_i$ content observed in *vip1* alleles defective in the phosphatase-like domain is unclear, but the contrasting $P_i$-related phenotypes between these *vip1* alleles and *ipk1-1* indicates that the decreased level of Ins$P_8$ in *ipk1* mutants is not responsible for $P_i$ homeostasis misregulation.

**ITPK1 and IPK1 constitute a pathway involved in the maintenance of $P_i$ homeostasis**

The common phenotypes observed in *itpk1* and *ipk1-1* mutants (i.e., excessive $P_i$ accumulation and elevated $P_i$ uptake under $P_i$-replete growth conditions) suggest that ITPK1 and IPK1 are involved in the same pathway that regulates $P_i$ homeostasis. Consistently, a common set of representative PSR genes was upregulated in *itpk1* and *ipk1-1* mutants (Figure 3a), and overexpression of *ITPK1* or *IPK1*

reduced shoot $P_i$ content (Figure 3b). Correspondingly, *ITPK1* overexpression significantly decreased $P_i$ uptake activity, in contrast to the elevated uptake activity shown by *itpk1* mutants (Figure 3c). In addition, several PSR genes were downregulated in *ITPK1*-overexpressing lines as compared with the WT (Figure 3a, e.g., *PHT1;2*, *SPX1*, *AT4*, *IPS1* and *PAP17*). However, $P_i$-uptake activity and PSR gene expression did not differ significantly between IPK1-overexpression lines and the WT (Figure 3a-d).

We drew additional support for the participation of ITPK1 and IPK1 in a common pathway regulating $P_i$ homeostasis in terms of their tissue-specific expression patterns and subcellular localization. Promoter-GUS activity assay and RT-PCR analysis demonstrated co-expression of *ITPK1* and *IPK1* throughout development and in specific tissues and cell types, such as vasculature, trichomes and guard cells (Figure 4a-k). In addition, neither gene was transcriptionally responsive to $P_i$ status (Figure 4l). The expression of ITPK1 native protein fused to yellow fluorescent protein (YFP), which restored $P_i$ content of the *itpk1* mutant to the WT level (Figure S4b), demonstrated co-localization of ITPK1 and IPK1 in the nucleus and cytoplasm (Figures 4m and S1c) (Kuo *et al.*, 2014).

We next examined the genetic interaction of *ITPK1* and *IPK1* with a genetic cross between *ipk1-1* and *itpk1* mutants. The *ipk1-1 itpk1* double mutants exhibited more severe growth defects than single mutants (Figure 4n) and those that proceeded to the reproductive stage bore aborted seeds [Figure 4n(iv'), (v')]. Tissue $P_i$ content was greater in *ipk1-1 itpk1* double than single mutants, by 50% to 70%, which is likely attributed to the relative 50% to 80% reduction in fresh weight (Figure 4o). Notably, expression of PSR genes in *ipk1-1 itpk1* double and single mutants was comparable (Figure 4p), which suggests IPK1 and ITPK1 function in a common regulatory pathway of $P_i$ homeostasis.

**A common elevation of D/L-Ins(3,4,5,6)$P_4$ in *itpk1* and *ipk1-1* mutants**

The observations that maintenance of $P_i$ homoeostasis depends on (1) the kinase activity of IPK1, (2) an additional Ins*P* kinase, ITPK1, and (3) the expression level of *ITPK1* and *IPK1* (i.e., contrary $P_i$-related phenotypes between mutants and overexpression lines), suggest the contribution of a stoichiometric alteration of Ins*P* metabolites to $P_i$ homeostasis regulation. To pinpoint the possible Ins*P* molecules involved in such regulation, we compared Ins*P* profiles of vegetative tissues of the relevant genotypes by *in vivo* labeling with [$^{32}$P]$P_i$ and/or *myo*-[$^3$H]inositol and HPLC analysis. As shown in Figure 5a, Figure 5b, and *myo*-[$^3$H]inositol-labeled chromatogram in Supporting Figure S6a, the *itpk1* mutant shared a significant reduction in Ins$P_6$ (62 ± 2% WT) with the *ipk1-1* mutant (17 ± 1% WT). To validate that reduced Ins$P_6$ level is not a cause of misregulated $P_i$ homeostasis, with the normal $P_i$-related phenotypes exhibited by another low-Ins$P_6$ mutant *mips1* (Murphy *et al.*, 2008; Kuo *et al.*, 2014), we analyzed the Ins*P* profile of the *mips1* mutant. Unexpectedly, *mips1* mutants exhibited a WT level of Ins$P_6$ (Figures 5a, b and S6a). For comparison, we also performed profile analysis of other *itpk* mutants and found that two *itpk4* mutants (*itpk4-1* and *itpk4-2*; Table S1) showed a strong reduction in Ins$P_6$ level comparable to *itpk1* and *ipk1-1* mutants, by 50% and 80%, respectively (Figures 5a, b and S6a). Consistent with the previous report, *itpk4* mutations also significantly reduced Ins$P_6$ level in seeds, to a similar extent as *ipk1-1* (Figure S7a) (Stevenson-Paulik *et al.*, 2005; Kim and Tai, 2011). The *itpk4* mutants did not show striking morphological phenotypes (Figures 2a and S3c) or $P_i$-related phenotypes, such as altered $P_i$ content (Figures 2b and S3e, S7b), $P_i$ uptake (Figure 2e), or altered PSR gene expression (Figure S7c). RT-PCR and promoter-GUS analysis indicated that *ITPK4* was expressed in the same vegetative tissues as *ITPK1* and *IPK1* (Figure S7d-l), which suggests that ITPK4 is likely involved in the same tissue-specific pool of Ins$P_6$ biosynthesis. In addition, YFP-tagged ITPK4, which complemented the seed-Ins$P_6$ phenotype of the *itpk4-1* mutant (Figure S7a), like ITPK1 and IPK1, was also localized to the nuclei and cytoplasm (Figure S7m). Hence,

reduced Ins$P_6$ level alone is insufficient to alter $P_i$ homeostasis and ITPK4 is a key enzyme for Ins$P_6$ biosynthesis in both vegetative tissues and seeds.

In accordance with decreased Ins$P_6$ level, Ins$P_7$ level was also decreased in the *ipk1-1* mutant (Figure 5a) (Laha *et al.*, 2015). Similarly, Ins$P_7$ level was decreased in *itpk1* and *itpk4* mutants (Figure 5a), and therefore we could not draw a correlation between the reduced Ins$P_7$ level and the $P_i$-related phenotypes observed in *ipk1-1* and *itpk1*. The *ipk1-1* mutant shows significant accumulation of Ins(1,3,4,5,6)$P_5$ along with reduced Ins$P_6$ level (Ins$P_{5b}$ in Figures 5a and S6a) (Stevenson-Paulik *et al.*, 2005), but in contrast, there was no detectable accumulation in the corresponding Ins$P_5$ in the *itpk1* mutant. This finding suggests that the elevated Ins(1,3,4,5,6)$P_5$ level in the *ipk1-1* mutant does not explain the misregulation of $P_i$ homeostasis.

Notably, the *itpk1* mutant showed elevated level of an Ins$P_4$ species with identical chromatographic mobility to that in the *ipk1-1* mutant, which is predominantly Ins(3,4,5,6)$P_4$ (Ins$P_4$* in Figures 5a and S6a) (Stevenson-Paulik *et al.*, 2005). The Ins$P_4$ species in the *itpk1* mutant was further analysed by high-resolution HPLC separation and was co-eluted with D/L-Ins(3,4,5,6)$P_4$ standard (D/L enantiomers are not separable by existing chromatographic technologies) (Figure 5c). In addition to the increase in Ins$P_4$ level, levels of earlier eluting Ins$P$ species were increased in both *itpk1* and *ipk1-1* mutants, which exhibited the chromatographic mobility of Ins$P_3$ (Figures 5a and S6a). Because there are 20 possible Ins$P_3$ isomers, being the most difficult Ins$P$ to resolve, isocratic HPLC analysis was performed under conditions designed for optimal resolution of these peaks (Wreggett and Irvine, 1989). As shown in Figure 5d, *ipk1-1* and *itpk1* mutations caused accumulation of distinct Ins$P_3$ isomers that were not detectable in the WT. Inclusion of an internal standard of *myo*-[$^3$H]Ins(1,4,5)$P_3$ revealed that these isomers are not Ins(1,4,5)$P_3$, which was shown to present only a trivial fraction of Ins$P_3$ in plant tissues (Brearley and Hanke, 2000). We conclude that the only common change of Ins$P$ species associated with the $P_i$-related phenotypes of *ipk1-1* and *itpk1* is the elevated D/L-Ins(3,4,5,6)$P_4$ level.

**$P_i$ starvation induced a shoot-specific increase of Ins*P*$_7$**

To address whether *itpk1* and *ipk1-1* mutants exhibit an Ins*P* profile that shares a common feature with $P_i$-starvation responses, we investigated the change in Ins*P* profiles in shoots and roots of WT plants in response to different $P_i$-starvation regimes. Ins*P* profiles were analyzed in seedlings subjected to 1- and 3-day $P_i$ starvation, when cellular $P_i$ concentrations were significantly reduced and PSR genes induced (Figure S8a, b). To avoid unequal [$^{32}$P]$P_i$ labeling between Pi-replete (supplemented with 250 µM Pi) and Pi-deficient (supplemented with 10 µM Pi) conditions and subsequent biased-quantifications of Ins*P*s, we performed a pulse-chase experiment with seedlings labeled with [$^{32}$P]$P_i$ before $P_i$ starvation. Tissues were similarly radiolabeled in every pairwise '+P' *vs*. '-P' treatment, although more [$^{32}$P] was allocated to shoots than roots (Figure 6a, b).

Overall, the chromatograms did not exhibit prominent profile changes in response to $P_i$ starvation in either shoots or roots (Figures 6a and S9). Quantitative analysis indicated no significant change in Ins$P_6$ level in response to $P_i$ starvation in shoots or roots (Figure 6c). Despite no significant change in Ins$P_7$ level in roots, shoots exhibited mild yet significant increase in Ins$P_7$-to-Ins$P_6$ ratio and Ins$P_7$ level in response to 1- and 3-day $P_i$ starvation (Figure 6d, e). We were unable to assess the Ins$P_8$ level due to the detection limit in our analysis; however, depletion of Ins$P_8$ caused by *vih2* mutation not affecting the $P_i$-starvation response implied that this Ins*P* species does not mediate $P_i$ signaling (Figure S5c). Notably, the increase in D/L-Ins(3,4,5,6)$P_4$ level in *itpk1* and *ipk1-1* mutants was not observed in $P_i$-starved WT plants (Figures 6f, g and S9a-d), nor was the level of any Ins$P_3$ isomer, including Ins(1,4,5)$P_3$, changed in response to $P_i$ starvation (Figure S9e, f).

Because cellular adenylate energy is influenced by $P_i$ availability (Boer *et al.*, 2010; Alexova *et al.*, 2017; Choi *et al.*, 2017), and high energy phosphates delivered by ATP are required for pyrophosphorylation (Voglmaier *et al.*, 1996), we examined whether phosphorylated adenine nucleotides are metabolically coordinated with the change in Ins$P_7$ level in response to $P_i$ starvation

by LC/MS analysis. ATP increased along with Ins$P_7$ level specifically in shoots during 1- and 3-day $P_i$ starvation, whereas AMP level remained steady (Figure 6h, I), which resulted in a significant increase of ATP/AMP ratio (0.68 ± 0.1 and 1.1 ± 0.1 for 3-day '+P' and '-P' treatment, respectively, $P$=0.009). In conclusion, the changes in Ins*P* profiles of WT seedlings in response to 1- and 3-day $P_i$ starvation distinctly differ from those in *itpk1* and *ipk1-1* mutants, which suggests that the mechanism of the ITPK1 and IPK1 contribution to $P_i$ homeostasis is distinct from the $P_i$-starvation response in WT plants.

## Discussion

In this study, we demonstrated metabolism of distinct Ins*P* species in correlation to $P_i$ homeostasis and $P_i$ limitation as summarized in Figure 7. Under $P_i$-replete conditions, the catalytic activity of IPK1 was required for maintenance of $P_i$ homeostasis, providing the first evidence of the involvement of Ins*P* metabolism, as opposed to other possible aspects of IPK1 protein function (Figures 1 and S1). This notion is further supported by the identification of an additional Ins*P*-synthesizing enzyme, ITPK1, with a comparable role to IPK1 (Figures 2, 3, S3 and S4). The epistatic relationship of *IPK1* and *ITPK1* in suppressing PSR genes under $P_i$-replete conditions, together with their co-expression pattern throughout development and their subcellular co-localization (Figure 4), indicate that ITPK1 and IPK1 constitute an Ins*P* metabolic pathway maintaining $P_i$ homeostasis. Ins*P* profiling revealed two distinct common features between *ipk1-1* and *itpk1* mutants: (1) decreases in Ins$P_6$ and Ins$P_7$ levels and (2) an increase in D/L-Ins(3,4,5,6)$P_4$ level (Figures 5 and S6). In contrast, $P_i$ starvation induced a distinct Ins*P* profile from those with *ipk1-1* and *itpk1* mutations (Figure 6), which suggests that *ipk1-1* and *itpk1* mutations affect $P_i$ homeostasis by a mechanism other than $P_i$-starvation signaling.

**Decrease in Ins$P_6$, Ins$P_7$ or Ins$P_8$ level is not responsible for disturbed $P_i$ homeostasis in *ipk1-1* and *itpk1* mutants**

The fact that *itpk4* mutants did not exhibit $P_i$-related phenotypes comparable to *ipk1-1* and *itpk1* mutants indicates that a decrease in Ins$P_6$ or Ins$P_7$ level did not cause the disturbed $P_i$ homeostasis under $P_i$-replete conditions. The similar tissue/developmental expression pattern and subcellular localization of ITPK4 as ITPK1 and IPK1 suggest that these three enzymes control the same pool of vegetative Ins$P_6$ and Ins$P_7$ (Figure S7). While it is possible that radiolabeling does not entirely reflect metabolic (subcellular) pools of different Ins*P* and PP-Ins*P* metabolites, no other methods have been elaborated for measurement of these molecules in plants, never mind their subcellular fractionation. Although we were unable to determine the Ins$P_8$ level, *vih2* mutants mediating Ins$P_8$ synthesis *in planta* (Laha *et al.*, 2015) did not phenocopy *ipk1-1* and *itpk1* under $P_i$-replete conditions and exhibited normal $P_i$-starvation responses (Figures 2, S3 and S5), which suggests that Ins$P_8$ is unlikely involved in the regulation of $P_i$ homeostasis.

We have also ruled out that misregulated $P_i$ homeostasis is a secondary consequence of mitigated Ins$P_6$-mediated mRNA export by demonstrating that mutations compromising or enhancing Ins$P_6$-Gle1-Los4 mRNA machinery neither caused comparable $P_i$-related phenotypes of *ipk1-1* nor complemented *ipk1-1* (Figure S2). The identification of two *itpk4* alleles with similar reduction in Ins$P_6$ (and Ins$P_7$) level in *ipk1-1* and *itpk1*, respectively, without showing $P_i$-related phenotypes, also argues against a role for Ins$P_6$-mediated mRNA export in regulating $P_i$ homeostasis (Figures 2, 5 and S7). Of note, although growth retardation of *ipk1-1* is attributed to defective Ins$P_6$-mediated mRNA export (Lee *et al.*, 2015), *itpk4* mutants did not exhibit growth defects comparable to *ipk1-1* or *itpk1* (Figure 2a). Thus, Ins$P_6$ reduction may not be the sole cause for the growth defect observed in the *ipk1-1* and *itpk1* mutants.

**Correlation between the increased level of D/L-Ins(3,4,5,6)$P_4$ and misregulation of $P_i$ homeostasis in *ipk1-1* and *itpk1* mutants**

Aside from the reduced levels of Ins$P_6$ and Ins$P_7$, the most significant common Ins*P* profile change between *itpk1* and *ipk1-1* is the increased accumulation of the Ins$P_4$ species, shown to predominantly consist of Ins(3,4,5,6)$P_4$ in the *ipk1-1* mutant (Stevenson-Paulik *et al.*, 2005). The isomeric identity of the Ins$P_4$ species in the *itpk1* mutant remains to be determined, but human ITPK1 was found a reversible Ins*P* 1-kinase/phosphatase that regulates the level of Ins(3,4,5,6)$P_4$, an inhibitor of $Ca^{2+}$-activated chloride channels in the plasma membrane (Vajanaphanich *et al.*, 1994; Yang *et al.*, 1999; Ho *et al.*, 2002; Saiardi and Cockcroft, 2008). In tobacco, Ins(3,4,5,6)$P_4$ is also linked to chloride transport, regulating growth and cell volume in pollen tubes (Zonia *et al.*, 2002). We attempted to test the effect of Ins(1,4,5,6)$P_4$ or Ins(3,4,5,6)$P_4$ on $P_i$ homeostasis of Arabidopsis seedlings by using membrane-permeant bioactivatable analogues of these two Ins*P* isomers [Bt2-Ins(1,4,5,6)$P_4$/PM and Bt2-Ins(3,4,5,6)$P_4$/PM] (Vajanaphanich *et al.*, 1994) but did not observe significant effects on tissue $P_i$ accumulation or PSR gene expression. However, the effectiveness of intracellular delivery and metabolism of these Ins*P* analogs on plant tissues remains to be assessed.

In addition to Ins$P_4$, Ins$P_3$ showed changes in *ipk1-1* and *itpk1* mutants (Figure 5d). In plants, Ins(1,4,5)$P_3$ (assayed by a competitive Ins$P_3$-receptor binding assay) has been linked to several physiological responses, such as gravitropism, salt and drought stresses (Perera *et al.*, 2001; Xiong *et al.*, 2001; Perera *et al.*, 2006; Perera *et al.*, 2008). We demonstrated that neither *ipk1-1* nor *itpk1* mutation affected the levels of Ins(1,4,5)$P_3$, as measured by radiolabelling approaches. Species that co-elute with this isomer are barely detectable in WT plants (Figure 5d) (Brearley and Hanke, 2000). Because the two mutants showed distinctive Ins$P_3$ profiles, and neither accumulated Ins(1,4,5)$P_3$, we did not find any association between changes in specific Ins$P_3$ and Pi homeostasis.

Because Ins*P* lipids, called polyphosphoinositides (PPIs), also play important roles in cellular signaling and Ins*P* metabolism (Munnik and Vermeer, 2010; Munnik and Nielsen, 2011), we examined whether PPI levels were altered in *ipk1-1* and *itpk1* mutants and found elevated levels of phosphatidylinositol 4,5-bisphosphate [PtdIns(4,5)$P_2$] in both *ipk1-1* and *itpk1* (Figure S10a, b). We further examined $P_i$-related phenotypes in mutants or transgenic lines with elevated levels of PtdIns$P_2$, i.e., *phosphatidylinositol-phospholipase C2* (*plc2*), *suppressor of actin 9* (*sac9*), and a *PHOSPHATIDYLINOSITOL PHOSPHATE 5-KINASE 3* (*PIP5K3*)-overexpression line (Williams *et al.*, 2005; Kusano *et al.*, 2008; Stenzel *et al.*, 2008; Kanehara *et al.*, 2015). None of these lines were comparable to the *ipk1-1* mutant (Figure S10c, d), which suggests that the increased PtdIns(4,5)$P_2$ levels in *ipk1-1* and *itpk1* mutants are not likely attributable to the misregulated $P_i$ homeostasis.

**$P_i$ starvation induced a change in Ins*P* profile distinct from those caused by *itpk1* and *ipk1-1* mutations**

Although *ipk1-1* and *itpk1* mutants exhibited characteristic phenotypes of $P_i$-starvation responses under $P_i$-replete conditions, their Ins*P* profiles were distinct from those under $P_i$ starvation, notably the contrasting levels of D/L-Ins(3,4,5,6)$P_4$, Ins$P_6$ and Ins$P_7$ (Figures 5a, 6f, 6g and S9a-d). The level of D/L-Ins(3,4,5,6)$P_4$ not being altered by $P_i$ starvation suggests these Ins*P* species are not involved in $P_i$-starvation signaling in WT plants. The disparate Ins*P* profiles in response to $P_i$ starvation versus that caused by *ipk1-1* and *itpk1* mutations imply two distinct $P_i$ signaling pathways. In support of this notion, the $P_i$-starvation responses persisted in the *ipk1-1* and *itpk1* mutants, in which PSR genes remained inducible under $P_i$ starvation (Figure S8c). We observed no distinct alteration of Ins*P* profile in response to $P_i$ starvation except for a significant increase in Ins$P_7$ level of unknown isomeric identity in the shoot of $P_i$-starved plants but not in the root (Figure 6d, e), where $P_i$-starvation responses also take place. Shoot tissues are more responsive to $P_i$ starvation than are roots (Huang *et al.*, 2008; Lin *et al.*, 2008), which has led to a hypothesis that the shoot is the tissue where $P_i$ starvation is sensed and the signal initiated (Hammond and White, 2008; Lin *et al.*, 2008).

Alternatively, because $P_i$ starvation triggers differential transcriptional and metabolic responses between shoots and roots (Wu *et al.*, 2003; Pant *et al.*, 2015), the shoot-specific increase in Ins$P_7$ level may have tissue-specific physiological significance under $P_i$ starvation conditions. It will be important to identify the kinase responsible for Ins$P_7$ synthesis in plants to address these speculations.

Adenylate energy has been shown to regulate PP-Ins*P*s synthesis, with increased ATP/ADP ratio promoting mammalian IP6K kinase activity (Wundenberg *et al.*, 2014). We observed that the shoot-specific increase in Ins$P_7$ level was associated with a shoot-specific increase in ATP and ATP/AMP ratio during 1- and 3-day $P_i$ starvation (Figure 6h, i). Increases in ATP level in response to $P_i$ starvation has been noted in barley leaves (Alexova *et al.*, 2017), which contrasts with the decrease in ATP level during $P_i$ starvation reported in yeast (Boer *et al.*, 2010; Choi *et al.*, 2017). $P_i$ starvation-induced ATP decreases have been shown in other plant species (Duff *et al.*, 1989; Rao *et al.*, 1989), but concentration ratios of ATP to ADP (or AMP), which control kinetics of cellular metabolism (Pradet and Raymond, 1983), remained unchanged or was increased in those studies. Whether the elevated ATP/AMP ratio drives Ins$P_7$ accumulation in $P_i$-starved shoots awaits further characterization of the Ins$P_7$ synthesis enzyme. Of note, multiple enzymes involved in adenine nucleotide metabolism have been genetically identified to act upstream of the Pho80/Pho85/Pho81 complex as negative regulators of PHO signaling (Huang and Shea, 2005; Choi *et al.*, 2017). Despite the inter-species difference in strategies for the $P_i$-starvation response, accumulating evidence has pointed to a close relationship between adenylate energy status and $P_i$ signaling. PP-Ins*P*s are proposed to be 'metabolic messengers' that mediate pyrophosphorylation of proteins involved in multiple cellular metabolism, including phosphorylation-based signal transduction pathways in yeast (Saiardi, 2012; Wu *et al.*, 2016). Whether the shoot-specific $P_i$ starvation-stimulated Ins$P_7$ observed in this study has a role in $P_i$ signaling by such protein pyrophosphoryaltion remains speculative.

**Significant roles of ITPK family of enzymes in phytate biosynthesis in plant vegetative tissues**

Mutation of *IPK1* leads to substantively reduced Ins$P_6$ level in seeds (Stevenson-Paulik *et al.*, 2005) and vegetative tissues (Stevenson-Paulik *et al.*, 2005; Nagy *et al.*, 2009). The concomitant accumulation of Ins(1,3,4,5,6)$P_5$ in these tissues/organs (Stevenson-Paulik *et al.*, 2005; Nagy *et al.*, 2009) strongly indicates the dominant contribution of the Ins(1,3,4,5,6)$P_5$ 2-kinase activity of IPK1 to Ins$P_6$ synthesis. The coincident accumulation of Ins(3,4,5,6)$P_4$ in vegetative tissues and seeds (Stevenson-Paulik *et al.*, 2005) may be explained by mass action effects (Hanke *et al.*, 2012), possibly indicating reversibility of the detected Ins(3,4,5,6)$P_4$ 1-kinase activity (Brearley and Hanke, 2000). The enzyme(s) responsible for producing Ins(3,4,5,6)$P_4$ in plants are not well defined. In avian erythrocytes, Ins(3,4,5,6)$P_4$ is the product of 5-phosphorylation of Ins(3,4,6)$P_3$ and is itself the precursor of Ins(1,3,4,5,6)$P_5$ (Stephens and Downes, 1990).

In nucleated mammalian cells, the origins of Ins(3,4,5,6)$P_4$ have not been tested by the methods of Stephens and Downes (Stephens and Downes, 1990), but the single mammalian ITPK1 is a multifunctional kinase and phosphotransferase that interconverts Ins(3,4,5,6)$P_4$ and Ins(1,3,4,5,6)$P_5$ (Chamberlain *et al.*, 2007). The existence in Arabidopsis of a gene family of four inositol tris/tetrakisphosphate kinases (ITPK1-4) complicates study of Ins*P* metabolism. Our identification of significant contributions of ITPK1 and ITPK4 to Ins$P_6$ synthesis in vegetative tissues focuses attention on the contribution of these enzymes to not just Ins$P_6$ synthesis but also physiological processes regulated by the intermediate Ins*P*s. *ITPK1* mutation reduces labeling of Ins$P_6$ by 50%, with concomitant accumulation of D/L-Ins(3,4,5,6)$P_4$, but because it does so without affecting Ins(1,3,4,5,6)$P_5$ level (Figures 5a and S6a) suggests that ITPK1 does not likely act as an Ins(1,3,4,5,6)$P_5$ 1-phosphatase. ITPK1 may be acting at the level of Ins$P_4$-Ins$P_5$ interconversion. Remarkably, our studies show that ITPK4, which contributes to nearly 90% of vegetative Ins$P_6$, and more in seeds, has no effect on the $P_i$-starvation response. Our labeling studies showed no increased Ins$P_4$ accumulation in vegetative tissues (Figures 5a and S6a). This implies that most of the Ins$P_4$

precursors for Ins$P_6$ synthesis are generated by this enzyme and the contribution of ITPK4 may lie in its Ins$P_3$ kinase activity rather than its Ins$P_4$ isomerase/mutase activity (Sweetman *et al.*, 2007).

**Implication of Ins*P* metabolism in regulating $P_i$ homeostasis**

Across eukaryotic kingdoms, the SPX domains of a large family of proteins involved in $P_i$ sensing and transport have been shown to bind Ins*P*s, thereby regulating SPX-protein activities and their interaction with other proteins (Wild *et al.*, 2016). Although Ins$P_6$ and PP-Ins*P*s at sub-micromolar concentration exhibited the highest binding affinity to the SPX domains, the lower Ins*P* levels also exhibited physiologically relevant binding affinity at a micromolar range (Wild *et al.*, 2016). Our study has pointed to a significant association between the level of D/L-Ins(3,4,5,6)$P_4$ and maintenance of $P_i$ homeostasis under $P_i$-replete conditions but not the $P_i$-starvation response. It remains speculative how increases in Ins$P_4$ level is associated with elevated $P_i$ uptake and PSR-gene expression and the future identification of the enantiomerism of D/L-Ins(3,4,5,6)$P_4$ in the *itpk1* mutant and its interacting protein targets, such as by using Ins*P* affinity screens (Wu *et al.*, 2016), should provide further mechanistic insights. The confounding effects on PHO signaling of Kcs1p (negative) and Vip1p (positive) (Auesukaree *et al.*, 2005; Lee *et al.*, 2007), together with a Vip1-indepdent $P_i$-starvation signaling pathway (Choi *et al.*, 2017), suggest the regulatory mechanisms that control $P_i$ homeostasis likely involve multiple Ins*P* and PP-Ins*P* species. Different Ins*P* and PP-Ins*P* species may regulate $P_i$ homeostasis via their competitive interaction with a spectrum of SPX-domain protein(s). For example, the binding of Ins$P_6$ and 5-Ins$P_7$ to OsSPX4/OsPHR2 yielded $K_d$ of ~ 50 µM and 7 µM respectively (Wild *et al.*, 2016), suggesting that competition between the more abundant Ins$P_6$ and less abundant PP-Ins*P*s are relevant considerations in SPX function (Wild *et al.*, 2016). Consequently, it will be important to consider the prevailing physiological concentration of potential Ins*P* and PP-Ins*P* competitors. Together with the diverse functions of SPX proteins at different levels of $P_i$ homeostasis regulation (Secco *et al.*, 2012; Azevedo and Saiardi,

2017) and our findings presented here, Ins$P_7$ may not be a general (or conserved) signal, and the role of other Ins*P* intermediates in regulating $P_i$ homeostasis need to be considered.

## Experimental procedures

### Plant materials and growth conditions

*Arabidopsis thaliana* mutant lines and their sources are listed in S1 Table; the wild-type line (WT) indicates Col-0 unless specified otherwise. Seeds were surface-sterilized, stratified at 4˚C for 1-3 days, and germinated on agar medium of half-strength modified Hoagland nutrient solution containing 250 µM $KH_2PO_4$, 1% sucrose, and 0.8% Bacto agar (Aung *et al.*, 2006). The $P_i$-replete ('+P') and $P_i$-deficient ('-P') media were supplemented with 250 µM (or 1 mM as specified) and 10 µM $KH_2PO_4$, respectively. For hydroponic growth, seedlings were germinated and grown on solid media for 10 days before being transferred to half-strength modified Hoagland nutrient solution with sucrose omitted. Plants were grown at 22 ˚C under a 16-h photoperiod with cool fluorescent white light at 100 to 150 µE $m^{-2}$ $s^{-1}$. For generating *ipk1-1 itpk1* double mutants, both double mutants and isogenic WT progenies were recovered from the F2 population at an equivalent yet lower segregation rate (1%) than expected (6%). Because these two loci are located on different arms of chromosome 5, the reason for this segregation distortion is unknown.

### Measurement of $P_i$ content and $P_i$ uptake activity

Total $P_i$ content and $P_i$ uptake activity were measured as described previously (Chiou *et al.*, 2006). To measure the root-to-shoot $P_i$ translocation activity, pulse-chase labeling was performed. 14-day after germination seedlings were first incubated in $P_i$-replete nutrient solution (half-strength modified Hoagland solution supplemented with 250 µM $KH_2PO_4$) containing $^{33}$[P]orthophosphate ($P_i$) for 3 h ('pulse' treatment), then transferred to $P_i$-replete nutrient solution without $^{33}$[P]$P_i$ for

indicated times ('chase' treatment). [$^{33}$P] radioactivity in the plants tissues was measured as the $P_i$ uptake assay and the root-to-shoot $P_i$ translocation activity was measured by shoot-to-root ratio of $^{33}$P count.

**Genotype analysis, transgene construction and plant transformation**

Primers used for genotyping of T-DNA insertional lines were designed according to SIGnAL (http://signal.salk.edu/tdnaprimers.2.html) and are listed in Supporting Table S2. For constructing kinase-inactive IPK1, nucleotide substitutions were introduced in the primers (5' phosphorylated; Supporting Table S2) used for PCR amplification by using a vector (pMDC32) containing the IPK1 CDS sequence driven by the 35S promoter as template. PCR product was ligated before transformation and sequences were confirmed before recombination into the Gateway destination vector pK7YWG2.0 (C'-YFP) (Karimi *et al.*, 2007) via LR Clonase enzyme mix (Invitrogen). For complementation analysis, the genomic sequence of ITPK1, including 1 kb upstream of ATG start codon, was amplified by PCR (primers listed in Supporting Table S2) and cloned into pCR8/GW/TOPO (Invitrogen) followed by recombination into the Gateway destination vectors. pMDC99, pMDC32 (Curtis and Grossniklaus, 2003), and pK7YWG2.0 were chosen as destination vectors for complementation, promoter::GUS activity and YFP fluorescence analysis, respectively. All cloned constructs were validated by sequencing analysis before being introduced into Arabidopsis by the floral-dip transformation method (Clough and Bent, 1998).

**RNA isolation, RT-PCR, and qRT-PCR**

Total RNA was isolated by using RNAzol reagent (Molecular Research Center) and cDNA was synthesized from 0.5 to 1 µg total RNA by using Moloney Murine Leukemia Virus Reverse Transcriptase (M-MLV RT, Invitrogen) and oligo(dT) primers. Sequences of primers used for RT-PCR and qRT-PCR are in Supporting Table S2. qRT-PCR involved use of the Power SYBR Green PCR Master Mix kit (Applied Biosystems) on a 7500 Real-Time PCR system as instructed. Gene expression was

normalized by subtracting the Ct value of *UBQ10* (ΔCt) from that of the gene studied and presented as $2^{-\Delta Ct}$. The expression relative to the WT (i.e., fold change relative to the WT) is presented as $2^{-\Delta\Delta Ct}$ (where $\Delta\Delta Ct = \Delta Ct - \Delta Ct^{WT}$). qPCR raw data is provided in Supporting Table S3.

**GUS staining and fluorescence microscopy**

GUS activity of transgenic T2 plants was detected as described (Lin *et al.*, 2005), and the signal was observed under an Olympus SZX12 or a Zeiss AxioSkop microscope. Confocal microscopy images of the YFP signal were obtained by using a Zeiss LSM 510 META NLO DuoScan with LCI Plan-Neofluar ×63/1.3 Immersion and Plan-Apochromat ×100/1.4 oil objectives. Excitation/emission wavelengths were 514 nm/520 to 550 nm for YFP.

**Ins*P* profiling of Arabidopsis seedlings and seeds**

For Ins*P* profile analysis of Arabidopsis vegetative tissue, seedlings (8-11 DAG) were labelled with *myo*-[2-$^{3}$H]inositol (19.6 Ci mmol$^{-1}$, Perkin Elmer NET114A00; 0.4 mCi mL$^{-1}$ for 5 days) or [$^{32}$P]$P_i$ (8500-9120Ci mmol$^{-1}$, Perkin Elmer NEX05300; 0.02 mCi mL$^{-1}$ for 1-3 days accordingly) in half-strength Hoagland's medium supplemented with $P_i$ at levels specified in the text. Ins*P* was extracted from the radiolabeled tissues, roots, shoots or whole seedlings as described (Azevedo and Saiardi, 2006). Extracts were resolved on a 250 x 4.6 mm Whatman Partisphere SAX WVS column fitted with guard cartridge of the same material at a flow rate of 1 mL min$^{-1}$ with a gradient derived from buffer reservoirs containing A, water; B, 1.25M $(NH_4)_2HPO_4$, adjusted to pH 3.8 with $H_3PO_4$, mixed according to the following gradient: time (min), %B; 0, 0; 5, 0; 65, 100; 75, 100. Isocratic separations of Ins$P_3$ species were performed at the same flow rate on the same column eluted with 20% buffer B. For *myo*-[$^{3}$H]inositol labeling, fractions were collected every minute from retention time 0 to 30 min and every 0.5 min from 30 min onward, followed by scintillation counting (1:4 ratio column eluent to scintillation cocktail; Perkin-Elmer; ULTIMA-FLO AP). For [$^{32}$P]$P_i$ labeling,

radioactivity was measured by Cherenkov counting on a Canberra Packard Radiomatic A515 Flow Detector fitted with a 0.5-mL flow cell with an integration interval of 0.1 min (Brearley *et al.*, 1997).

*myo*-[$^{3}$H]inositol and [$^{32}$P]$P_i$ exhibited different allocation between tissues *in planta*, with greater [$^{3}$H] labeling of roots (Figure S6b), whereas [$^{32}$P]$P_i$ labeled shoots more strongly (Figure 6b). With the exception of experiments to compare the extent of labeling of Ins$P_6$ between a wide range of genotypes (Figure 5b), performed with whole seedlings, the shoot and root tissues were analyzed independently. Aside from stoichiometric differences of specific Ins*P*s, the Ins*P* profile was in general similar between these two tissues (Figures 6a and S6b).

For analysis of Ins*P*s in seeds, 2 mg seed was homogenized in 500 µl of ice-cold 0.6 N HCl before centrifugation for 15 min to remove cell debris. Aliquots (20 µL) were injected onto a 3 mm i.d. x 200 mm Carbo Pac PA200 HPLC column (Dionex) fitted with a 3 mm x 50 mm guard column of the same material. The column was eluted at a flow rate of 0.4 mL/min with a gradient of methane sulfonic acid (Acros Organics) delivered from buffer reservoirs containing: A, water; B, 600 mM methane sulfonic acid according to the following schedule: time (minutes), % B; 0, 0; 25, 100; 38, 100; 39, 0; 49, 0. The column eluate was mixed by using a mixing tee with a solution of 0.1% w/v ferric nitrate in 2% w/v perchloric acid (Phillippy and Bland, 1988) delivered at a flow rate of 0.2 mL/min, before passage through a 194-uL volume knitted reaction coil (4 m x 0.25 mm i.d.) obtained from Biotech AB, Sweden. The column, mixing tee and reaction coil were held at 35°C. Peaks of Ins*P* were detected at 290 nm with a Jasco UV-2077 Plus UV detector. Chromatographic data were integrated in ChromNav (Jasco) software. The position of elution of different stereoisomers of the different classes of Ins*P*s was determined by the inclusion at regular intervals of a set of standards obtained by extended acid treatment of phytic acid (middle panel in Figure 5c).

**ATP and AMP analysis**

Adenylates from plant tissues were extracted as described (Cho *et al.*, 2016). Tissues were homogenized in liquid nitrogen and re-suspended in 2.3% (v/v) TCA containing 200 µg/ml ribitol (250 µl per 100 mg tissue). Homogenates were centrifuged at 13,000 rpm at 4°C for 15 min, and supernatants were recovered and neutralized to pH 6.5-7 by KOH, followed by 30-min incubation on ice. Extracts were centrifuged at 13,000 rpm at 4°C for 15 min and the supernatants were collected for LC/MS quantification with an ultra-performance liquid chromatography (UPLC) system (ACQUITY UPLC, Waters, Millford, MA). The sample was separated with a ZIC-cHILIC column (3-µm particle size, 2.1 × 100 mm, Merck-Millipore). The UPLC system was coupled online to the Waters Xevo TQ-S triple quadruple mass spectrometer. Ribitol was used as internal standard. Characteristic MS transitions were monitored by the negative multiple reaction monitoring (MRM) mode for ATP (m/z, 506→159), AMP (m/z, 346→79), and ribitol (m/z, 151→71). Data acquisition and processing involved use of MassLynx v4.1 and TargetLynx software (Waters Corp.), with intensities of ATP and AMP normalized to ribitol.

## Acknowledgements

We thank Shu-Chen Shen (Confocal Microscope Facility, Scientific Instrument Center, Academia Sinica, Taiwan) for fluorescence microscopy imaging, Chen-Chuan Hsu (Plant Tech Core Facility, ABRC, Academia Sinica, Taiwan) for cross-section imaging of GUS staining in plants, ABRC Metabolomics Core for LC-MS measurement of ATP/AMP, Hsin-Yu Huang, Su-Fen Chiang and Hayley Whitfield (University of East Anglia, Norwich, United Kingdom) for technical support. *vih* and *plc2* mutants were kindly given by Gabriel Schaff (University of Bonn, Germany) and Kazue Kanehara (Institute of Plant and Microbial Biology, Academia Sinica, Taipei, Taiwan), respectively; mutants and transgenic lines of Gle1-Los4 mRNA export machinery were generously provided by Ho-Seok Lee and

Hyun-Sook Pai (Department of Systems Biology, Yonsei University, Seoul, Korea). This work was supported by grants from the Ministry of Science and Technology of the Republic of China (MOST 104-2321-B-001-057, MOST 105-2321-B-001-038 and MOST 106-2321-B-001-026 to T.-J. Chiou and postdoctoral fellowship to H.-F. Kuo), the BBSRC grants from the United Kingdom (BB/M022978/1 and BB/N002024/1 to C.A. Brearley), and the Netherlands Organization for Scientific Research (NWO 867.15.020 and 711.017.005 to T. Munnik).

## Conflict of Interest

The authors declare no conflict of interest.

## Author Contributions

H.-F.K. and T.-J.C. conceived the project; H.-F.K., C.B. and T.-J.C. designed the experiments; H.-F.K., Y.-Y.H., W.-C.L., K.-Y.C., T.M. and C.B. performed the research; H.-F.K., C.B., T.M. and T.-J.C. interpreted the results; H.-F.K. and C.B. wrote the manuscript; H.-F.K., T.M., C.B. and T.-J.C. contributed to the final version of this article.

## Supporting Information

## References

**Alcazar-Roman, A.R., Tran, E.J., Guo, S. and Wente, S.R.** (2006) Inositol hexakisphosphate and Gle1 activate the DEAD-box protein Dbp5 for nuclear mRNA export. *Nat. Cell Biol.*, **8**, 711-716.

**Alexova, R., Nelson, C.J. and Millar, A.H.** (2017) Temporal development of the barley leaf metabolic response to Pi limitation. *Plant Cell Environ.*, **40**, 645-657.

**Auesukaree, C., Tochio, H., Shirakawa, M., Kaneko, Y. and Harashima, S.** (2005) Plc1p, Arg82p, and Kcs1p, enzymes involved in inositol pyrophosphate synthesis, are essential for phosphate regulation and polyphosphate accumulation in Saccharomyces cerevisiae. *J. Biol. Chem.*, **280**, 25127-25133.

**Aung, K., Lin, S.I., Wu, C.C., Huang, Y.T., Su, C.L. and Chiou, T.J.** (2006) *pho2*, a phosphate overaccumulator, is caused by a nonsense mutation in a microRNA399 target gene. *Plant Physiol.*, **141**, 1000-1011.

**Azevedo, C. and Saiardi, A.** (2017) Eukaryotic phosphate homeostasis: the inositol pyrophosphate perspective. *Trends Biochem Sci*, **42**, 219-231.

**Bari, R., Datt Pant, B., Stitt, M. and Scheible, W.R.** (2006) PHO2, microRNA399, and PHR1 define a phosphate-signaling pathway in plants. *Plant Physiol.*, **141**, 988-999.

**Berridge, M.J.** (2009) Inositol trisphosphate and calcium signalling mechanisms. *Biochim. Biophys. Acta.*, **1793**, 933-940.

**Boer, V.M., Crutchfield, C.A., Bradley, P.H., Botstein, D. and Rabinowitz, J.D.** (2010) Growth-limiting intracellular metabolites in yeast growing under diverse nutrient limitations. *Mol. Biol. Cell*, **21**, 198-211.

**Bosch, D. and Saiardi, A.** (2012) Arginine transcriptional response does not require inositol phosphate synthesis. *J. Biol. Chem.*, **287**, 38347-38355.

**Brearley, C.A. and Hanke, D.E.** (1993) Pathway of synthesis of 3,4- and 4,5-phosphorylated phosphatidylinositols in the duckweed *Spirodela polyrhiza* L.. *Biochem J*, **290 ( Pt 1)**, 145-150.

**Brearley, C.A. and Hanke, D.E.** (1996) Metabolic evidence for the order of addition of individual phosphate esters in the myo-inositol moiety of inositol hexakisphosphate in the duckweed *Spirodela polyrhiza* L.. *Biochem J*, **314 ( Pt 1)**, 227-233.

**Brearley, C.A. and Hanke, D.E.** (2000) Metabolic relations of inositol 3,4,5,6-tetrakisphosphate revealed by cell permeabilization. Identification of inositol 3,4,5,6-tetrakisphosphate 1-kinase and inositol 3,4,5,6-tetrakisphosphate phosphatase activities in mesophyll cells. *Plant Physiol.*, **122**, 1209-1216.

**Brearley, C.A., Parmar, P.N. and Hanke, D.E.** (1997) Metabolic evidence for PtdIns(4,5)$P_2$-directed phospholipase C in permeabilized plant protoplasts. *Biochem. J.*, **324 ( Pt 1)**, 123-131.

**Chamberlain, P.P., Qian, X., Stiles, A.R., Cho, J., Jones, D.H., Lesley, S.A., Grabau, E.A., Shears, S.B. and Spraggon, G.** (2007) Integration of inositol phosphate signaling pathways via human ITPK1. *J. Biol. Chem.*, **282**, 28117-28125.

**Chiou, T.-J. and Lin, S.-I.** (2011) Signaling network in sensing phosphate availability in plants. *Annu. Rev. Plant Biol.*, **62**, 185-206.

**Chiou, T.J., Aung, K., Lin, S.I., Wu, C.C., Chiang, S.F. and Su, C.L.** (2006) Regulation of phosphate homeostasis by microRNA in Arabidopsis. *Plant Cell*, **18**, 412-421.

**Cho, H.-Y., Wen, T.-N., Wang, Y.-T. and Shih, M.-C.** (2016) Quantitative phosphoproteomics of protein kinase SnRK1 regulated protein phosphorylation in Arabidopsis under submergence. *J. Exp. Bot.*, **67**, 2745-2760.

**Choi, J., Rajagopal, A., Xu, Y.-F., Rabinowitz, J.D. and O'Shea, E.K.** (2017) A systematic genetic screen for genes involved in sensing inorganic phosphate availability in *Saccharomyces cerevisiae*. *PLoS ONE*, **12**, e0176085.

**Clough, S.J. and Bent, A.F.** (1998) Floral dip: a simplified method for Agrobacterium-mediated transformation of *Arabidopsis thaliana*. *Plant J.*, **16**, 735-743.

**Curtis, M.D. and Grossniklaus, U.** (2003) A gateway cloning vector set for high-throughput functional analysis of genes in planta. *Plant Physiol.*, **133**, 462-469.

**Desai, M., Rangarajan, P., Donahue, J.L., Williams, S.P., Land, E.S., Mandal, M.K., Phillippy, B.Q., Perera, I.Y., Raboy, V. and Gillaspy, G.E.** (2014) Two inositol hexakisphosphate kinases drive inositol pyrophosphate synthesis in plants. *Plant J.*, **80**, 642-653.

**Duff, S.M., Moorhead, G.B., Lefebvre, D.D. and Plaxton, W.C.** (1989) Phosphate starvation inducible 'bypasses' of adenylate and phosphate dependent glycolytic enzymes in *Brassica nigra* suspension cells. *Plant Physiol.*, **90**, 1275-1278.

**Franco-Zorrilla, J.M., Martin, A.C., Leyva, A. and Paz-Ares, J.** (2005) Interaction between phosphate-starvation, sugar, and cytokinin signaling in Arabidopsis and the roles of cytokinin receptors CRE1/AHK4 and AHK3. *Plant Physiol.*, **138**, 847-857.

**Gonzalez, B., Banos-Sanz, J.I., Villate, M., Brearley, C.A. and Sanz-Aparicio, J.** (2010) Inositol 1,3,4,5,6-pentakisphosphate 2-kinase is a distant IPK member with a singular inositide binding site for axial 2-OH recognition. *Proc. Natl. Acad. Sci. USA*, **107**, 9608-9613.

**Hammond, J.P. and White, P.J.** (2008) Sucrose transport in the phloem: integrating root responses to phosphorus starvation. *J. Exp. Bot.*, **59**, 93-109.

**Hanke, D.E., Parmar, P.N., Caddick, S.E., Green, P. and Brearley, C.A.** (2012) Synthesis of inositol phosphate ligands of plant hormone-receptor complexes: pathways of inositol hexakisphosphate turnover. *Biochem. J.*, **444**, 601-609.

**Ho, M.W.Y., Yang, X., Carew, M.A., Zhang, T., Hua, L., Kwon, Y.-U., Chung, S.-K., Adelt, S., Vogel, G., Riley, A.M., Potter, B.V.L. and Shears, S.B.** (2002) Regulation of Ins(3,4,5,6)$P_4$ signaling by a reversible kinase/phosphatase. *Curr. Biol.*, **12**, 477-482.

**Holford, I.C.R.** (1997) Soil phosphorus: its measurement, and its uptake by plants. *Soil Res.*, **35**, 227-240.

**Huang, C.Y., Roessner, U., Eickmeier, I., Genc, Y., Callahan, D.L., Shirley, N., Langridge, P. and Bacic, A.** (2008) Metabolite profiling reveals distinct changes in carbon and nitrogen metabolism in phosphate-deficient barley plants (*Hordeum vulgare* L.). *Plant Cell Physiol.*, **49**, 691-703.

**Huang, S. and Shea, E.K.** (2005) A systematic high-throughput screen of a yeast deletion collection for mutants defective in PHO5 regulation. *Genetics*, **169**, 1859.

**Irvine, R.F. and Schell, M.J.** (2001) Back in the water: the return of the inositol phosphates. *Nat. Rev. Mol. Cell Biol.*, **2**, 327-338.

**Kanehara, K., Yu, C.Y., Cho, Y., Cheong, W.F., Torta, F., Shui, G., Wenk, M.R. and Nakamura, Y.** (2015) Arabidopsis AtPLC2 is a primary phosphoinositide-specific phospholipase C in phosphoinositide metabolism and the endoplasmic reticulum stress response. *PLoS Genet.*, **11**, e1005511.

**Karimi, M., Depicker, A. and Hilson, P.** (2007) Recombinational cloning with plant gateway vectors. *Plant Physiol.*, **145**, 1144-1154.

**Kim, S.I. and Tai, T.H.** (2011) Identification of genes necessary for wild-type levels of seed phytic acid in *Arabidopsis thaliana* using a reverse genetics approach. *Mol. Genet. Genomics*, **286**, 119-133.

**Kuo, H.F., Chang, T.Y., Chiang, S.F., Wang, W.D., Charng, Y.Y. and Chiou, T.J.** (2014) Arabidopsis inositol pentakisphosphate 2-kinase, AtIPK1, is required for growth and modulates phosphate homeostasis at the transcriptional level. *Plant J.*, **80**, 503-515.

**Kusano, H., Testerink, C., Vermeer, J.E.M., Tsuge, T., Shimada, H., Oka, A., Munnik, T. and Aoyama, T.** (2008) The Arabidopsis phosphatidylinositol phosphate 5-kinase PIP5K3 is a key regulator of root hair tip growth. *Plant Cell*, **20**, 367-380.

**Laha, D., Johnen, P., Azevedo, C., Dynowski, M., Weiss, M., Capolicchio, S., Mao, H., Iven, T., Steenbergen, M., Freyer, M., Gaugler, P., de Campos, M.K., Zheng, N., Feussner, I., Jessen, H.J., Van Wees, S.C., Saiardi, A. and Schaaf, G.** (2015) VIH2 regulates the synthesis of inositol pyrophosphate $InsP_8$ and jasmonate-dependent defenses in Arabidopsis. *Plant Cell*, **27**, 1082-1097.

**Lee, H.-S., Lee, D.-H., Cho, H.K., Kim, S.H., Auh, J.H. and Pai, H.-S.** (2015) $InsP_6$-sensitive variants of the Gle1 mRNA export factor rescue growth and fertility defects of the *ipk1* low-phytic-acid mutation in Arabidopsis. *Plant Cell*, **27**, 417-431.

**Lee, Y.S., Huang, K., Quiocho, F.A. and O'Shea, E.K.** (2008) Molecular basis of cyclin-CDK-CKI regulation by reversible binding of an inositol pyrophosphate. *Nat. Chem. Biol.*, **4**, 25-32.

**Lee, Y.S., Mulugu, S., York, J.D. and O'Shea, E.K.** (2007) Regulation of a cyclin-CDK-CDK inhibitor complex by inositol pyrophosphates. *Science*, **316**, 109-112.

**Lemtiri-Chlieh, F., MacRobbie, E.A. and Brearley, C.A.** (2000) Inositol hexakisphosphate is a physiological signal regulating the $K^+$-inward rectifying conductance in guard cells. *Proc. Natl. Acad. Sci. USA*, **97**, 8687-8692.

**Lemtiri-Chlieh, F., MacRobbie, E.A., Webb, A.A., Manison, N.F., Brownlee, C., Skepper, J.N., Chen, J., Prestwich, G.D. and Brearley, C.A.** (2003) Inositol hexakisphosphate mobilizes an endomembrane store of calcium in guard cells. *Proc. Natl. Acad. Sci. USA*, **100**, 10091-10095.

**Lin, S.I., Chiang, S.F., Lin, W.Y., Chen, J.W., Tseng, C.Y., Wu, P.C. and Chiou, T.J.** (2008) Regulatory network of microRNA399 and PHO2 by systemic signaling. *Plant Physiol.*, **147**, 732-746.

**Lin, S.I., Wang, J.G., Poon, S.Y., Su, C.L., Wang, S.S. and Chiou, T.J.** (2005) Differential regulation of *FLOWERING LOCUS C* expression by vernalization in cabbage and Arabidopsis. *Plant Physiol.*, **137**, 1037-1048.

**Lin, W.-Y., Huang, T.-K. and Chiou, T.-J.** (2013) NITROGEN LIMITATION ADAPTATION, a target of microRNA827, mediates degradation of plasma membrane–localized phosphate transporters to maintain phosphate homeostasis in Arabidopsis. *Plant Cell*, **25**, 4061-4074.

**Liu, J., Samac, D.A., Bucciarelli, B., Allan, D.L. and Vance, C.P.** (2005) Signaling of phosphorus deficiency-induced gene expression in white lupin requires sugar and phloem transport. *Plant J.*, **41**, 257-268.

**Liu, J., Yang, L., Luan, M., Wang, Y., Zhang, C., Zhang, B., Shi, J., Zhao, F.-G., Lan, W. and Luan, S.** (2015) A vacuolar phosphate transporter essential for phosphate homeostasis in Arabidopsis. *Proc. Natl. Acad. Sci. USA*, **112**, E6571-E6578.

**Liu, T.-Y., Huang, T.-K., Yang, S.-Y., Hong, Y.-T., Huang, S.-M., Wang, F.-N., Chiang, S.-F., Tsai, S.-Y., Lu, W.-C. and Chiou, T.-J.** (2016) Identification of plant vacuolar transporters mediating phosphate storage. *Nat. Commun.*, **7**.

**Lonetti, A., Szijgyarto, Z., Bosch, D., Loss, O., Azevedo, C. and Saiardi, A.** (2011) Identification of an evolutionarily conserved family of inorganic polyphosphate endopolyphosphatases. *J. Biol. Chem.*, **286**, 31966-31974.

**Müller, R., Nilsson, L., Krintel, C. and Hamborg Nielsen, T.** (2004) Gene expression during recovery from phosphate starvation in roots and shoots of *Arabidopsis thaliana*. *Physiol. Plantarum*, **122**, 233-243.

**Martin, A.C., del Pozo, J.C., Iglesias, J., Rubio, V., Solano, R., de La Pena, A., Leyva, A. and Paz-Ares, J.** (2000) Influence of cytokinins on the expression of phosphate starvation responsive genes in Arabidopsis. *Plant J.*, **24**, 559-567.

**Mosblech, A., Konig, S., Stenzel, I., Grzeganek, P., Feussner, I. and Heilmann, I.** (2008) Phosphoinositide and inositolpolyphosphate signalling in defense responses of *Arabidopsis thaliana* challenged by mechanical wounding. *Mol. Plant*, **1**, 249-261.

**Mulugu, S., Bai, W., Fridy, P.C., Bastidas, R.J., Otto, J.C., Dollins, D.E., Haystead, T.A., Ribeiro, A.A. and York, J.D.** (2007) A conserved family of enzymes that phosphorylate inositol hexakisphosphate. *Science*, **316**, 106-109.

**Munnik, T.** (2014) PI-PLC: phosphoinositide-phospholipase C in plant signaling. In *Signaling and Communication in Plants* (Wang, X. ed.). Berlin Heidelberg: Springer-Verlag, pp. 27-54.

**Munnik, T. and Nielsen, E.** (2011) Green light for polyphosphoinositide signals in plants. *Curr. Opin. Plant Biol.*, **14**, 489-497.

**Munnik, T. and Vermeer, J.E.M.** (2010) Osmotic stress-induced phosphoinositide and inositol phosphate signalling in plants. *Plant Cell Environ.*, **33**, 655-669.

**Murphy, A.M., Otto, B., Brearley, C.A., Carr, J.P. and Hanke, D.E.** (2008) A role for inositol hexakisphosphate in the maintenance of basal resistance to plant pathogens. *Plant J.*, **56**, 638-652.

**Nagy, R., Grob, H., Weder, B., Green, P., Klein, M., Frelet-Barrand, A., Schjoerring, J.K., Brearley, C. and Martinoia, E.** (2009) The Arabidopsis ATP-binding cassette protein AtMRP5/AtABCC5 is a high affinity inositol hexakisphosphate transporter involved in guard cell signaling and phytate storage. *J. Biol. Chem.*, **284**, 33614-33622.

**Norbis, F., Boll, M., Stange, G., Markovich, D., Verrey, F., Biber, J. and Murer, H.** (1997) Identification of a cDNA/Protein Leading to an Increased P i -uptake in *Xenopus laevis* Oocytes. *J.Membrane Biol.* **156**, 19-24.

**Pant, B.-D., Pant, P., Erban, A., Huhman, D., Kopka, J. and Scheible, W.-R.** (2015) Identification of primary and secondary metabolites with phosphorus status-dependent abundance in Arabidopsis, and of the transcription factor PHR1 as a major regulator of metabolic changes during phosphorus limitation. *Plant Cell Environ.*, **38**, 172-187.

**Perera, I.Y., Heilmann, I., Chang, S.C., Boss, W.F. and Kaufman, P.B.** (2001) A role for inositol 1,4,5-trisphosphate in gravitropic signaling and the retention of cold-perceived gravistimulation of oat shoot pulvini. *Plant Physiol.*, **125**, 1499-1507.

**Perera, I.Y., Hung, C.Y., Brady, S., Muday, G.K. and Boss, W.F.** (2006) A universal role for inositol 1,4,5-trisphosphate-mediated signaling in plant gravitropism. *Plant Physiol.*, **140**, 746-760.

**Perera, I.Y., Hung, C.Y., Moore, C.D., Stevenson-Paulik, J. and Boss, W.F.** (2008) Transgenic Arabidopsis plants expressing the type 1 inositol 5-phosphatase exhibit increased drought tolerance and altered abscisic acid signaling. *Plant Cell*, **20**, 2876-2893.

**Phillippy, B.Q. and Bland, J.M.** (1988) Gradient ion chromatography of inositol phosphates. *Anal. Biochem.*, **175**, 162-166.

**Pradet, A. and Raymond, P.** (1983) Adenine nucleotide ratios and adenylate energy charge in energy metabolism. *Ann. Rev. Plant Physio.*, **34**, 199-224.

**Puga, M.I., Mateos, I., Charukesi, R., Wang, Z., Franco-Zorrilla, J.M., de Lorenzo, L., Irigoyen, M.L., Masiero, S., Bustos, R., Rodriguez, J., Leyva, A., Rubio, V., Sommer, H. and Paz-Ares, J.** (2014) SPX1 is a phosphate-dependent inhibitor of Phosphate Starvation Response 1 in Arabidopsis. *Proc. Natl. Acad. Sci. USA*, **111**, 14947-14952.

**Raboy, V.** (1997) Accumulation and storage of phosphate and minerals. In *Cellular and Molecular Biology of Plant Seed Development* (Larkins, B.A. and Vasil, I.K. eds): Kluwer Academic Publishers, pp. 441-477.

**Raboy, V.** (2003) *myo*-Inositol-1,2,3,4,5,6-hexakisphosphate. *Phytochemistry*, **64**, 1033-1043.

**Rao, I.M., Arulanantham, A.R. and Terry, N.** (1989) Leaf phosphate status, photosynthesis and carbon partitioning in sugar beet: II. Diurnal changes in sugar phosphates, adenylates, and nicotinamide nucleotides. *Plant Physiol.*, **90**, 820-826.

**Rouached, H., Arpat, A.B. and Poirier, Y.** (2010) Regulation of phosphate starvation responses in plants: signaling players and cross-talks. *Mol. Plant*, **3**, 288-299.

**Saiardi, A.** (2012) Cell signalling by inositol pyrophosphates. *Sub-cell. Biochem.*, **59**, 413-443.

**Saiardi, A. and Cockcroft, S.** (2008) Human ITPK1: a reversible inositol phosphate kinase/phosphatase that links receptor-dependent phospholipase C to $Ca^{2+}$-activated chloride channels. *Sci. Signal.*, **1**, pe5.

**Saiardi, A., Erdjument-Bromage, H., Snowman, A.M., Tempst, P. and Snyder, S.H.** (1999) Synthesis of diphosphoinositol pentakisphosphate by a newly identified family of higher inositol polyphosphate kinases. *Curr. Biol.*, **9**, 1323-1326.

**Schell, M.J., Letcher, A.J., Brearley, C.A., Biber, J., Murer, H. and Irvine, R.F.** (1999) $P_i$US ($P_i$ uptake stimulator) is an inositol hexakisphosphate kinase. *FEBS Lett.*, **461**, 169-172.

**Schneider, S.** (2015) Inositol transport proteins. *FEBS Lett.*, **589**, 1049-1058.

**Secco, D., Wang, C., Arpat, B.A., Wang, Z., Poirier, Y., Tyerman, S.D., Wu, P., Shou, H. and Whelan, J.** (2012a) The emerging importance of the SPX domain-containing proteins in phosphate homeostasis. *New Phytol.*, **193**, 842-851.

**Secco, D., Wang, C., Shou, H. and Whelan, J.** (2012b) Phosphate homeostasis in the yeast *Saccharomyces cerevisiae*, the key role of the SPX domain-containing proteins. *FEBS Lett.*, **586**, 289-295.

**Shears, S.B., Ganapathi, S.B., Gokhale, N.A., Schenk, T.M.H., Wang, H., Weaver, J.D., Zaremba, A. and Zhou, Y.** (2012) Defining signal transduction by inositol phosphates. *Sub-cell. Biochem.*, **59**, 389-412.

**Stenzel, I., Ischebeck, T., König, S., Hołubowska, A., Sporysz, M., Hause, B. and Heilmann, I.** (2008) The type B phosphatidylinositol-4-phosphate 5-kinase 3 is essential for root hair formation in *Arabidopsis thaliana*. *Plant Cell*, **20**, 124-141.

**Stephens, L.R. and Downes, C.P.** (1990) Product-precursor relationships amongst inositol polyphosphates. Incorporation of [$^{32}$P]$P_i$ into myo-inositol 1,3,4,6-tetrakisphosphate, *myo*-inositol 1,3,4,5-tetrakisphosphate, *myo*-inositol 3,4,5,6-tetrakisphosphate and *myo*-inositol 1,3,4,5,6-pentakisphosphate in intact avian erythrocytes. *Biochem. J.*, **265**, 435-452.

**Stephens, L.R. and Irvine, R.F.** (1990) Stepwise phosphorylation of *myo*-inositol leading to *myo*-inositol hexakisphosphate in Dictyostelium. *Nature*, **346**, 580-583.

**Stevenson-Paulik, J., Bastidas, R.J., Chiou, S.T., Frye, R.A. and York, J.D.** (2005) Generation of phytate-free seeds in Arabidopsis through disruption of inositol polyphosphate kinases. *Proc. Natl. Acad. Sci. USA*, **102**, 12612-12617.

**Stevenson-Paulik, J., Odom, A.R. and York, J.D.** (2002) Molecular and biochemical characterization of two plant inositol polyphosphate 6-/3-/5-kinases. *J. Biol. Chem.*, **277**, 42711-42718.

**Sweetman, D., Stavridou, I., Johnson, S., Green, P., Caddick, S.E. and Brearley, C.A.** (2007) *Arabidopsis thaliana* inositol 1,3,4-trisphosphate 5/6-kinase 4 (AtITPK4) is an outlier to a family of ATP-grasp fold proteins from Arabidopsis. *FEBS Lett.*, **581**, 4165-4171.

**Szijgyarto, Z., Garedew, A., Azevedo, C. and Saiardi, A.** (2011) Influence of inositol pyrophosphates on cellular energy dynamics. *Science*, **334**, 802-805.

**Torabinejad, J. and Gillaspy, G.E.** (2006) Functional genomics of inositol metabolism. In *Biology of Inositols and Phosphoinositides: Subcellular Biochemistry* (Majumder, A.L. and Biswas, B.B. eds). Boston, MA: Springer US, pp. 47-70.

**Vajanaphanich, M., Schultz, C., Rudolf, M.T., Wasserman, M., Enyedi, P., Craxton, A., Shears, S.B., Tsien, R.Y., Barrett, K.E. and Traynor-Kaplan, A.** (1994) Long-term uncoupling of chloride secretion from intracellular calcium levels by Ins(3,4,5,6)$P_4$. *Nature*, **371**, 711-714.

**Voglmaier, S.M., Bembenek, M.E., Kaplin, A.I., Dormán, G., Olszewski, J.D., Prestwich, G.D. and Snyder, S.H.** (1996) Purified inositol hexakisphosphate kinase is an ATP synthase: diphosphoinositol pentakisphosphate as a high-energy phosphate donor. *Proc. Natl. Acad. Sci. USA*, **93**, 4305-4310.

**Wang, Z., Ruan, W., Shi, J., Zhang, L., Xiang, D., Yang, C., Li, C., Wu, Z., Liu, Y., Yu, Y., Shou, H., Mo, X., Mao, C. and Wu, P.** (2014) Rice SPX1 and SPX2 inhibit phosphate starvation responses through interacting with PHR2 in a phosphate-dependent manner. *Proc. Natl. Acad. Sci. USA*, **111**, 14953-14958.

**Whiteford, C.C., Brearley, C.A. and Ulug, E.T.** (1997) Phosphatidylinositol 3,5-bisphosphate defines a novel PI 3-kinase pathway in resting mouse fibroblasts. *Biochem. J.*, **323 ( Pt 3)**, 597-601.

**Wild, R., Gerasimaite, R., Jung, J.Y., Truffault, V., Pavlovic, I., Schmidt, A., Saiardi, A., Jessen, H.J., Poirier, Y., Hothorn, M. and Mayer, A.** (2016) Control of eukaryotic phosphate homeostasis by inositol polyphosphate sensor domains. *Science*, **352**, 986-990.

**Williams, M.E., Torabinejad, J., Cohick, E., Parker, K., Drake, E.J., Thompson, J.E., Hortter, M. and Dewald, D.B.** (2005) Mutations in the Arabidopsis phosphoinositide phosphatase gene SAC9 lead to overaccumulation of PtdIns(4,5)$P_2$ and constitutive expression of the stress-response pathway. *Plant Physiol.*, **138**, 686-700.

**Wilson, M.P. and Majerus, P.W.** (1997) Characterization of a cDNA encoding *Arabidopsis thaliana* inositol 1,3,4-trisphosphate 5/6-kinase. *Biochem. Bioph. Res. Co.*, **232**, 678-681.

**Wreggett, K.A. and Irvine, R.F.** (1989) Automated isocratic high-performance liquid chromatography of inositol phosphate isomers. *Biochem. J.*, **262**, 997.

**Wu, M., Chong, L.S., Perlman, D.H., Resnick, A.C. and Fiedler, D.** (2016) Inositol polyphosphates intersect with signaling and metabolic networks via two distinct mechanisms. *Proc. Natl. Acad. Sci. USA*, **113**, E6757-E6765.

**Wu, P., Ma, L., Hou, X., Wang, M., Wu, Y., Liu, F. and Deng, X.W.** (2003) Phosphate starvation triggers distinct alterations of genome expression in Arabidopsis roots and leaves. *Plant Physiol.*, **132**, 1260-1271.

**Wundenberg, T., Grabinski, N., Lin, H. and Mayr, G.W.** (2014a) Discovery of $InsP_6$-kinases as $InsP_6$-dephosphorylating enzymes provides a new mechanism of cytosolic $InsP_6$ degradation driven by the cellular ATP/ADP ratio *Biochem. J.*, **462**, 173-184.

**Wundenberg, T., Grabinski, N., Lin, H. and Mayr, Georg W.** (2014b) Discovery of InsP6-kinases as InsP6-dephosphorylating enzymes provides a new mechanism of cytosolic InsP6 degradation driven by the cellular ATP/ADP ratio. *Biochem. J.*, **462**, 173-184.

**Xiong, L., Lee, B., Ishitani, M., Lee, H., Zhang, C. and Zhu, J.K.** (2001) FIERY1 encoding an inositol polyphosphate 1-phosphatase is a negative regulator of abscisic acid and stress signaling in Arabidopsis. *Gene. Dev.*, **15**, 1971-1984.

**Xu, R., Paul, B.D., Smith, D.R., Tyagi, R., Rao, F., Khan, A.B., Blech, D.J., Vandiver, M.S., Harraz, M.M., Guha, P., Ahmed, I., Sen, N., Gallagher, M. and Snyder, S.H.** (2013a) Inositol polyphosphate multikinase is a transcriptional coactivator required for immediate early gene induction. *Proc. Natl. Acad. Sci. USA*, **110**, 16181-16186.

**Xu, R., Sen, N., Paul, B.D., Snowman, A.M., Rao, F., Vandiver, M.S., Xu, J. and Snyder, S.H.** (2013b) Inositol polyphosphate multikinase is a coactivator of p53-mediated transcription and cell death. *Sci. Signal.*, **6**, ra22-.

**Yang, X., Rudolf, M., Carew, M.A., Yoshida, M., Nerreter, V., Riley, A.M., Chung, S.-K., Bruzik, K.S., Potter, B.V.L., Schultz, C. and Shears, S.B.** (1999) Inositol 1,3,4-trisphosphate acts in vivo as

a specific regulator of cellular signaling by inositol 3,4,5,6-tetrakisphosphate. *J. Biol. Chem.*, **274**, 18973-18980.

**Yang, X.J. and Finnegan, P.M.** (2010) Regulation of phosphate starvation responses in higher plants. *Ann. Bot.*, **105**, 513-526.

**York, J.D., Odom, A.R., Murphy, R., Ives, E.B. and Wente, S.R.** (1999) A phospholipase C-dependent inositol polyphosphate kinase pathway required for efficient messenger RNA export. *Science*, **285**, 96-100.

**Zonia, L., Cordeiro, S., Tupy, J. and Feijo, J.A.** (2002) Oscillatory chloride efflux at the pollen tube apex has a role in growth and cell volume regulation and is targeted by inositol 3,4,5,6-tetrakisphosphate. *Plant Cell*, **14**, 2233-2249.

## Figure legends

**Figure 1. Characterization of kinase-inactive IPK1 transgenic plants.**

(a) Relative $InsP_6$ content (% of WT) in seeds of *ipk1-1* mutants and homozygous transgenic lines expressing C-terminus YFP-tagged wild-type *IPK1* (*IPK1-YFP*), $IPK1^{K168A}$ ($IPK1^{K168A}$-*YFP*), or $IPK1^{D368A}$ ($IPK1^{D368A}$-*YFP*) coding sequences in the *ipk1-1* mutant background. Error bars, S.E. of n=3-12 independent experiments. (b) Relative expression (to WT) of PSR genes in roots, and (c) $P_i$ content in shoots of 14-days after germination (DAG) seedlings. Asterisks indicate significant differences from WT (Student's *t*-test; **, $P < 0.005$).

**Figure 2. Characterization of mutants defective in Ins*P* biosynthesis enzymes grown under $P_i$-replete condition.**

(a) Morphology of 22-DAG plants grown in $P_i$-replete (1 mM) hydroponic medium. Scale bar, 1 cm. (b) $P_i$ content in the shoots of 14-DAG seedlings grown on $P_i$-replete (1 mM) solid medium. Error bar, S.E. of n=4-21 independent experiments. (c-f) $P_i$ uptake activities of 14-DAG seedlings under $P_i$-replete (250 μM) growth conditions. Error bars, S.E. of n=3-24 independent experiments. Uptake

activities of genotypes in (a-c) were measured in overlapping sets of experiments and plotted separately for clear presentation. Asterisks denote significant differences from the WT (Student's *t*-test; **, $P < 0.005$).

**Figure 3. Phenotype similarities between *itpk1, ipk1-1* mutants, and overexpression lines.**

(a) Relative expression (to WT) of PSR genes in roots of 14-DAG *itpk1*, *ipk1*-1, *IPK1*-overexpression (*OxIPK1*) and *ITPK1*-overexpression (*OxITPK1*) lines grown under $P_i$-replete (1 mM) conditions (see Supporting Table S3 for qPCR raw data and S.E. of 3 independent experiments). Note that qPCR primers for *ITPK1* are located 5' to the T-DNA insertion site. (b) $P_i$ content in shoots of 14-DAG T2 transgenic lines overexpressing *ITPK1* or *IPK1* compared to WT, *itpk1* and *ipk1-1* mutants grown under $P_i$-replete (250 µM) condition. Error bars, S.E. of n=6-12 independent experiments. (c and d) $P_i$ uptake activities of 14-DAG seedlings grown under $P_i$-replete (250 µM $P_i$) condition. Error bars, S.E. of n=6-12 independent experiments. Asterisks denote significant differences from the WT (Student's *t*-test; **, $P < 0.005$).

**Figure 4. Tissue-specific expression and protein subcellular localization of ITPK1 and IPK1, and phenotypes of *itpk1*, *ipk1-1* and *itpk1 ipk1-1* double mutants.**

(a-j) Promoter activities of *IPK1* and *ITPK1* at different developmental stages. (a) 3-DAG; scale bar, 10 µm. (b) 5-DAG; scale bar, 1 mm. (c) 7-DAG; scale bar, 1 mm. (d) 14-DAG; scale bar, 1 cm. (e) Cross section of 14-DAG root; scale bar, 10 µm. (f) Guard cells of 14-DAG leaves; scale bar, 10 µm. (g) Trichome of 14-DAG leaves; scale bar, 0.1 mm. (h) 22-DAG floral tissues; scale bar, 0.5 cm. (i) 22-DAG flowers; scale bar, 0.5 mm. (j) Siliques; scale bar, 0.5 mm. (K and L) RT-PCR analysis of tissue-specific expression of *ITPK1* and *ITPK4* at different developmental stages (k) and in response to $P_i$ status (l). S, shoot; R, root; LF, rosette leaves; FS, florescence stem; FL, flower; SL, silique; +P, 250 µM $P_i$; -P, 10 µM $P_i$. PCR amplification cycles for *ITPK1*, 32; *ITPK4*, 32; *ACTIN2*, 22. (m) Subcellular localization of C-terminus YFP-tagged IPK1 and ITPK1 protein in roots of 10-DAG *ipk1-1* and *itpk1* mutants,

respectively; scale bar, 10 µm. Arrows, cytoplasm, arrowheads, nucleus. (n) Morphology of 25-DAG *itpk1 ipk1-1* mutants grown under $P_i$-replete (250 µM) conditions. Insets show enlarged images of floral tissues (i'), rosette leaves (ii'), roots (iii'), mature siliques (iv') and aborted seeds (v'). Scale bars are 1 cm, 1 mm and 100 µm for the whole plant, insets (a-d) and inset (e), respectively. (o) Tissue-specific $P_i$ content and (p) relative expression of PSR genes of 16-DAG seedlings grown on $P_i$-replete (250 µM) solid medium. Error bar, S.E. of n=3-6 independent experiments. Asterisks denote significant differences from the WT (Student's *t*-test; *, $P < 0.05$; **, $P < 0.005$).

**Figure 5. Ins*P* profiles of various genotypes.**

(a) HPLC analysis of roots extracts from 11-DAG seedlings of various genotypes labeled with [$^{32}$P]$P_i$. Ins$P_{5a}$, Ins(1,2,4,5,6)$P_5$ and/or Ins(2,3,4,5,6)$P_5$ and/or Ins(1,2,3,4,6)$P_5$ (these three isomers are not resolved on Partisphere SAX HPLC (Brearley and Hanke, 1996); Ins$P_{5b}$, Ins(1,3,4,5,6)$P_5$; Ins$P_4$*, Ins(1,4,5,6)$P_4$ and/or Ins(3,4,5,6)$P_4$; Ins$P_3$, peaks with the chromatographic mobility of Ins$P_{3s}$. Insets show expanded chromatograms of more polar Ins*P*s, obtained by counting 1-min fractions collected from the Flo-Detector eluted from retention time of 50 min onwards. The ordinate is scaled by the same factor for the different genotypes, representing a constant fraction of the largest ($P_i$) peak in each chromatogram. (b) Quantification of relative Ins$P_6$ content (% of total radioactivity per HPLC run recovered in the integrated Ins$P_6$ peak) in 11-DAG [$^{32}$P]$P_i$-labeled seedlings. Error bar, S.E. of n=3-5 independent experiments. Double asterisks denote a significant difference from the WT (Student's *t*-test, $P < 0.005$). (c) Identity of Ins$P_4$* in *itpk1* mutant. An aliquot of extract of [$^{32}$P]$P_i$-labeled *itpk1* seedlings (11-DAG) was spiked with a hydrolysate of Ins$P_6$ and separated on a CarboPac PA200 column with post-column colourimetric detection of Ins*P* peaks as described (Phillippy and Bland, 1988). Upper panel, [$^{32}$P]-radioactivity counted inline on the Flo Detector. Note that Ins$P_4$ and Ins$P_5$ are below the level of detection on the Flo Detector, and therefore corresponding fractions (0.5 min) were collected for static counting (lower panel). Middle panel, UV trace obtained from this extract. Ins(1,4,5,6)$P_4$/Ins(3,4,5,6)$P_4$ is the latest eluting Ins$P_4$ on this column

and elutes before Ins(1,2,3,4,6)$P_5$. Lower panel, UV trace overlaid with [$^{32}$P] counts of collected fractions. The retention time of the fractions in the upper and lower panel is corrected for the plumbing delay between the UV detector and the Flo Detector or the fraction collector. The broadness of the [$^{32}$P] peaks (compared to the sharp UV peaks) is a consequence of band broadening after the UV detector (in the Flo Detector and the collected fractions). All the other Ins$P_4$ isomers elute before 20 min. Ins$P_5$[5-OH], Ins(1,2,3,4,6)$P_5$; Ins$P_5$[4/6-OH], Ins(1,2,3,5,6)$P_5$ and/or Ins(1,2,3,4,5)$P_5$; Ins$P_5$[1/3-OH], Ins(1,2,4,5,6)$P_5$ and/or Ins(2,3,4,5,6)$P_5$; Ins$P_5$[2-OH], Ins(1,3,4,5,6)$P_5$. Note that a single peak of Ins$P_4$ was detected in *itpk1* in (a). (d) Isocratic separation and counting of collected fractions for analysis of Ins$P_3$ isomers. For better presentation, the chromatogram of each genotype was shifted by 200 CPM.

**Figure 6. Tissue-specific Ins*P* profiles in response to 1- and 3-day $P_i$ starvation**.

(a) Chromatograms of HPLC analysis of [$^{32}$P]$P_i$-labeled WT seedlings after 1- and 3-day $P_i$-replete (+P, 250 µM) or $P_i$-deficient (-P, 10 µM) treatments. 8-DAG seedlings were labeled with [$^{32}$P]$P_i$ under $P_i$-replete conditions for 3 days ("pulse") before transfer to unlabeled media ("chase"). Insets show enlarged chromatograms of more polar InsPs, plotted from scintillation counts of 1-min fractions collected from retention time 50 min onwards. For clearer presentation, [$^{32}$P] radioactivity signals of $P_i$ starvation treatment (S-P and R-P) were shifted by 100 CPM. Ins$P_{5a}$, Ins(1,2,4,5,6)$P_5$ and/or Ins(2,3,4,5,6)$P_5$. (b) Total [$^{32}$P]$P_i$ recovered in metabolites of tissues after pulse-chase labeling determined by integration of peaks from in-line flow detection. Error bars, SE of three independently labeled populations of seedlings. (c) Ins$P_6$ level as percentage of total radioactivity across the gradient recovered in the integrated peak. (d) Ins$P_7$-to-Ins$P_6$ ratio determined from counting of fractions in inset (a). (e) Ins$P_7$ level as per mille total radioactivity derived from Ins$P_7$-to-Ins$P_6$ ratio [derived in (d)] multiplied by the Ins$P_6$ level in (c). (f) Ins$P_4$*-to-Ins$P_6$ ratio determined by scintillation counting of fractions as shown in Supporting Figure S9A. Ins$P_4$* shares common retention time with the elevated peak detected in the *ipk1-1* and *itpk1* mutants (Figure 5). (g) Ins$P_4$* level as per mille

total radioactivity derived from Ins$P_4$*-to-Ins$P_6$ ratio (Figure S9A-D) multiplied by the Ins$P_6$ level in (c). Error bars in (b-g), S.E. of three independent labeling experiments. (h and i) Relative ATP and AMP level per mg fresh weight (FW) derived from normalization to the internal standard ribitol. Error bars, S.E. of n=9 and 7 independent experiments for the shoots and roots, respectively. Asterisks indicate significant differences from the WT (Student's *t*-test; *, $P < 0.05$).

**Figure 7. Intersections between Ins*P* metabolism and $P_i$ homeostasis.** Biochemical pathways for the synthesis of Ins$P_6$ and PP-Ins*P*s in vegetative tissues of Arabidopsis, consisting of a 'lipid-dependent pathway' based on biochemical activities of homologous enzymes (Raboy, 2003; Stevenson-Paulik *et al.*, 2003; Stevenson-Paulik *et al.*, 2005; Kim and Tai, 2011; Munnik and Nielsen, 2011; Desai *et al.*, 2014; Laha *et al.*, 2015) and 'lipid-independent pathway' identified in the duckweed *Spirodela polyrhiza* (Brearley and Hanke, 1993; Brearley *et al.*, 1997). For the 'alternative lipid-dependent pathway', an alternative substrate, PtdIns4*P*, for PLC is proposed based on enzyme's capacity to hydrolyse this lipid, the physiological levels *of* PtdIns4*P* while PtdIns(4,5)$P_2$ is hardly detectable, and the fact that plant PLCs lack a PH domain to bind PtdIns(4,5)$P_2$ (Munnik, 2014). The identity and origin of Ins$P_3$ substrate for ITPK4 is unknown. IMP, inositol monophosphatase; MIK, *myo*-inositol kinase; INT2 & 4, INOSITOL TRANSPORTER 2 & 4 (Schneider, 2015); PIS, phosphatidylinositol synthase; PI4K, phosphatidylinositol 4-kinase.

(a)

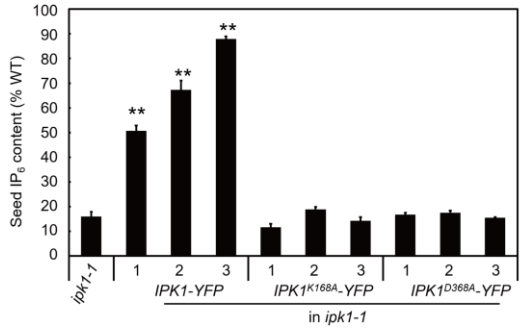


(b)

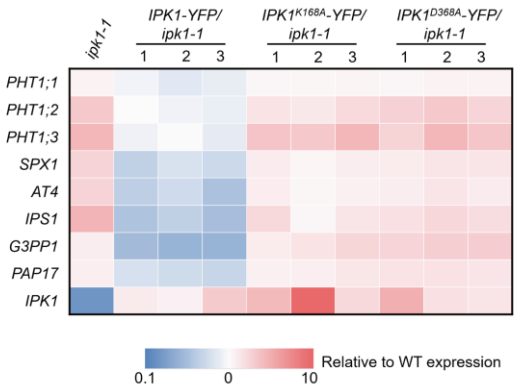


(c)